Project #: DJO - 0308

Design of a One Kilowatt Scale Kite Power System

A Major Qualifying Project Report
Submitted to the Faculty
of the
WORCESTER POLYTECHNIC INSTITUTE

in partial fulfillment of the requirements for the
Degree of Bachelor of Science
In Aerospace Engineering

SUBMITTED BY:

Ryan Buckley
rbuckley@wpi.edu

Max Hurgin
maxpower@wpi.edu

Chris Colschen
ccol86@wpi.edu

Erik Lovejoy
elovejoy@wpi.edu

Michael DeCuir
mgdecuir@wpi.edu

Nick Simone
nsimone@wpi.edu

Date: April 23rd, 2008

Professor David Olinger, Project Advisor

1 Abstract

The goal of this project was to design and build a one-kilowatt scale system for generating power using a kite. Kite power has the potential to be more economical than using wind turbines because kites can fly higher than turbines can operate. At higher altitudes, wind speeds and available power are increased. In the developed system, a large windboarding kite pulls the end of a long rocking arm which turns a generator and creates electricity. This motion is repeated using a mechanism that changes the angle of attack of the kite during each cycle, thus varying its lift force and allowing a rocking motion of the arm. The end of the arm turns a shaft with a flywheel attached and spins a mounted generator, whose output then gets stored in batteries for later use. A Matlab simulation was used to predict a power output for the system of approximately one kilowatt. All sub-components of the system (power conversion mechanism, angle of attack mechanism, and kite control mechanism) have been lab tested. The complete kite power system has been field tested to confirm that the system structure can withstand the structural loads imposed by the kite. The kite power system has produced power for short time intervals with the rocking arm restricted to a portion of its full range of motion. A future application for this system will be in a developing nation without access to a power grid.

2 Table of Contents

2.1 Table of Figures

3 Introduction

If current global energy consumption trends continue, rough estimates show that non-renewable energy sources could be depleted by as early as 2054[1]. These estimates are obviously not indicative of actual circumstances because as the energy sources diminish, consumption will presumably adjust to those conditions. However, it important to understand the inevitable fate of non-renewable energy; simply stated, it will run out. Renewable energy alternatives have thus become increasingly popular in the modern world. Among those alternatives, one largely untapped resource is wind power. In addition to being renewable, wind power is a clean energy source, not contributing to harmful byproducts such as carbon dioxide which may be contributing to global climate change. Figure 1 shows the increasing popularity of wind power, which is currently second only to hydropower, according to the Renewable Energy Policy Network[2].

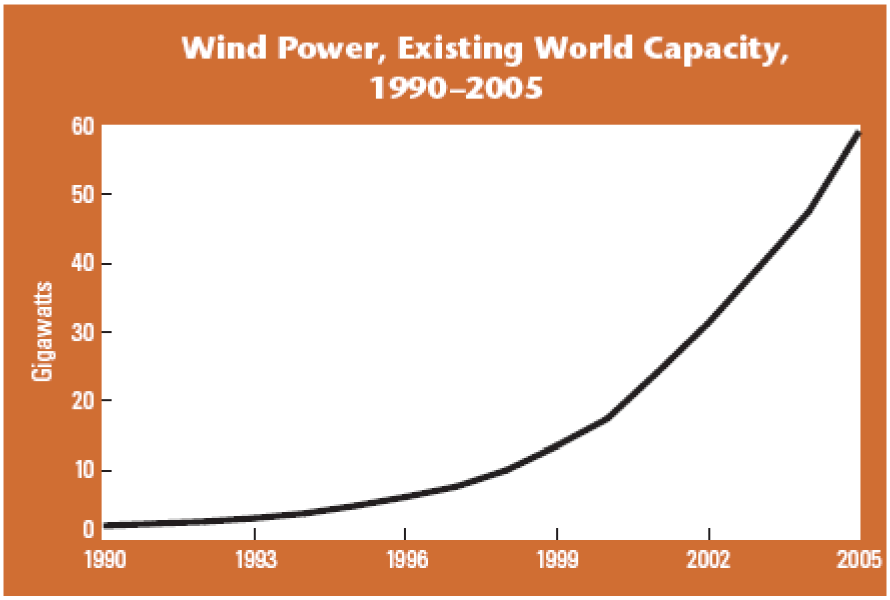

Figure 1: Global Wind Power Capacity[2]

Along with increasing global demand, the domestic demand for wind power is also increasing. Figure 2 shows that although the fraction of renewable energy consumption in the US has not significantly increased over the past 15 years, the fraction of wind energy consumption to total energy consumption *has* significantly increased. Furthermore, the fraction of wind energy within the renewable energy sector has also increased dramatically.

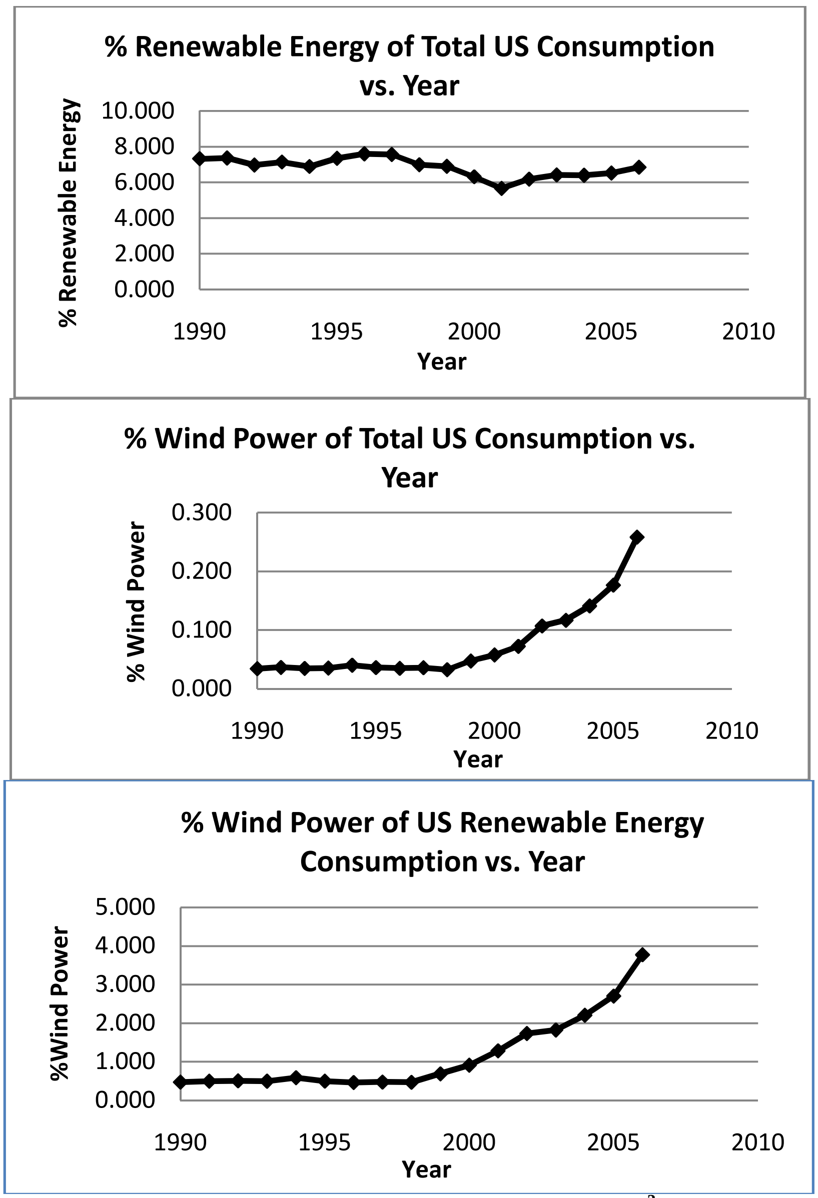

Figure 2: US Wind Consumption Statistics[3]

Wind turbines account for nearly one hundred percent of wind power being produced today. One major disadvantage of the wind turbine is that as the height is increased (to access higher wind velocities) the turbine blades become more difficult to structurally support, and manufacturing stronger towers can become increasingly expensive. Another significant downside to wind turbines that should not be overlooked is the noise that they produce. Nina Pierpont, MD, PhD, who is a wind turbine noise expert asserts that "it is critical that industrial wind turbines not be placed within a minimum of 1.5 miles of human dwellings."[4] Her studies show a vast array of medical and behavioral symptoms, which she even deems "Wind Turbine Syndrome", that arise in situations where people reside close to wind turbines. This effect obviously limits the locations in which they can be employed. In addition to the noise pollution, there is also visual pollution associated with wind turbines. Many people consider wind turbines to be aesthetically unpleasing, and there is strong opposition to many wind farm projects from land owners and nature conservation groups.[5]

An alternative to using wind turbines is using large kites to harness wind power. Perhaps the most significant advantage that kite power holds over turbine power is its performance at high altitudes. Equation 1 shows that wind speed increases following a 1/7th power law, where y is the height, V is velocity, and the subscript 0 indicates a reference condition.

$$\frac{V}{V_0} = \left(\frac{y}{y_0}\right)^{\frac{1}{7}} \qquad (1)$$

Since power increases proportionally to the cube of wind speed, higher altitude obviously results in greater power potential. Figure 3 shows the effect of altitude on wind speed and power.

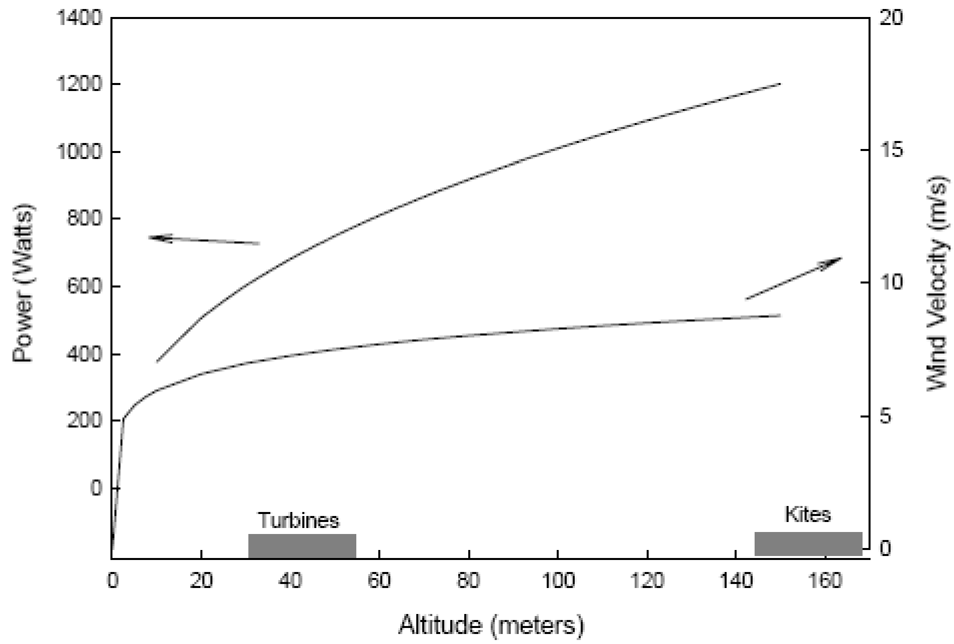

Figure 3: Power output and wind velocity for turbine and kite of 10 m^2 area[6]

Whereas turbine blades are held up by a rigid tower, a kite provides its own lift and is only attached to kite lines. Increasing the altitude of the kites merely implies increasing the length of the kite lines. Consequently, once a robust system of power harnessing with kites is achieved, accessing higher power at higher altitudes is simple and inexpensive. For example, flying a kite at 150m compared to operating a turbine at 50m would approximately double the available wind power.

The goal of our project is to design and build a prototype one kilowatt scale kite power system. An application of this kite power system would be in a rural area of a developing nation, specifically one that did not have or could not afford access to the main power grid. This project was started by an MQP team last year[7], and this year we built on their work to develop a functional prototype. The most difficult challenges of the project were to autonomously control the kite and to efficiently convert its movement into electrical energy. These tasks required both mechanical design prowess and a fundamental understanding of the kite's dynamics.

4 Background

Though kite powered wind energy has not until recently become a popular concept, its principles and potential have been considered for almost thirty years.

In 1979, Loyd[8] investigated the potential for kite powered energy. According to Loyd, G. Pocock had contemplated the use of kites to provide mechanical energy as far back as 1825 but was limited by lack of advancement in the field of aerodynamics at the time. Pocock's research did establish that kites were a feasible source of mechanical energy as he was able to move loads across the ground using only kite power with marginal effectiveness. Loyd built upon these concepts by developing systems of equations governing crosswind kite motion and applying them to modern airfoils. Extrapolating his results to technology similar to sophisticated wind turbines, Loyd estimated that a $2000m^2$ kite flying at 1200m could produce 45MW (for comparison, the average production of an industrial coal power plant is about 667MW).

At nearly the same time Dr J.S. Goela was conducting similar research at the Indian Institute of Technology Kanpur. While Dr. Goela published a number of yearly reports in the 70's and 80's, our project focused on concepts and theories explored in his reports from 1976[9], 1983[10], and 1986[11]. Specifically, our project is interested in the equation of kite motion and power outlined in Goela. The goal of this work was to "experimentally demonstrate that systems employing kites can be used to convert wind energy into useful mechanical energy."[11]

Goela mathematically analyzed the steady state motion of kites and developed equations to predict the kite's motion and power output. To do so, he broke the kite's cycle into two phases, the ascent and descent. During ascent the kite produces power. The power output during the ascent can be optimized for given conditions.

The effect of tether line drag on power output was also studied. Goela found that for the thick tethers being used for this application, both gravity and wind resistance must be included in determining the overall transmission efficiency (the ratio of tether tension at the kite to the tension experienced at the ground). In doing so, he noted that the tether's static profile and behavior vary significantly from a common catenary, but could actually be modeled as a straight line if shorter than 1000 meters and inclined 80^o or greater.

Experimentally, Goela intended to produce a mechanism to pump water using only kite-power. His research team first tested a number of kite designs before deciding on the "conyne" kite as the best for their models. The conyne kite is a triangular box kite with side wings as seen in Figure 4 and combines the stability advantage of box kites with the lifting capacity of flat kites. The team then tested a scale model conyne kite in a wind tunnel and determined tension in the model tether as a function of angle of attack.

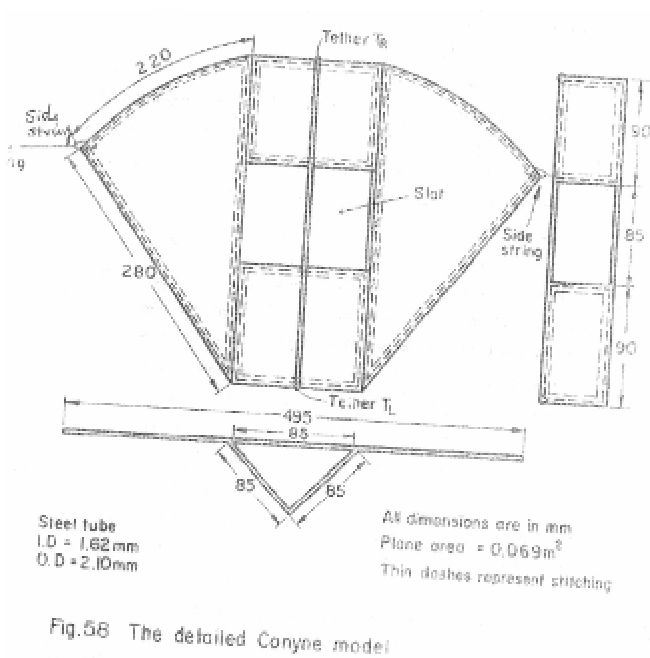

Figure 4: Conyne Kite from Goela, 1983

Goela's team also designed a mechanical device to raise a bucket of water from a well using the kite's lift and then lower the bucket by reducing the kite's angle of attack, and consequently lift. Goela's kite-pump mechanism was explained by the previous year's MQP as:

> The mechanism that Dr. Goela and his team designed consisted of a balanced beam on a fulcrum with spring-loaded assists as shown in Figure 4. The springs in the system were used as a switching mechanism in order to change the angle of attack of the kite, cycling from ascent to descent. As the balanced-beam reaches the top of its path, the water is discarded from the bucket, decreasing its weight bucket as the angle of attack is decreased with the flip of the lever. The motion described above is portrayed in the two stage view in Figure 5. Once the angle of attack is changed the bucket is slightly heavier than the tension in the tether and the kite is pulled back down to its starting point. The cycle restarts once the lever is triggered in the opposite direction during the descent of the bucket and kite.[7]

Dr Goela, whose research and designs have heavily influenced the WPI Wind Power from Kites project, has also lent his support as a technical consultant for this MQP. He has reviewed the work on the project and participated in field testing of the kite power system.

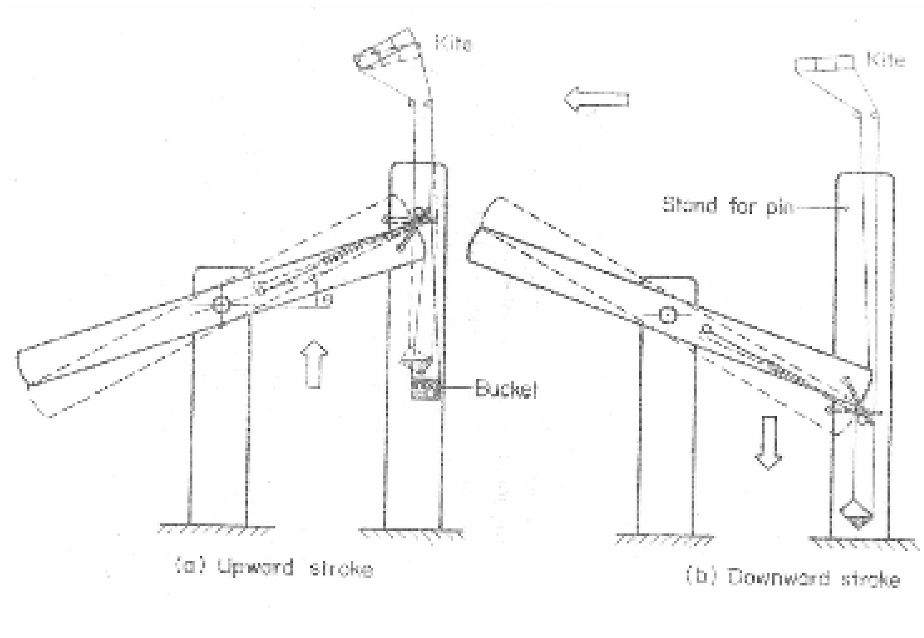

Figure 5: Goela Spring Model View 2, From Goela (1983)

Recently, the idea of kite powered energy generation is again being studied, however the focus is often on larger power (MW scale) systems with kites flying at higher altitudes. The Kite Gen group, based in Milan, Italy is currently working on a massive kite-driven power plant aiming to replace nuclear plants in the future. The Kite Gen design involves a number of kites tethered to a large ring. As the kites fly and produce power, the ring rotates about a shaft, producing mechanical energy. Kite Gen's kites are controlled by a system of winches attached to the tethers of each kite, driven by complex avionics software developed for this specific use. Kite Gen currently has plans for 100 MW and 1 GW plants.

In 2005 David D. Lang[12] performed a detailed analysis of six different kite powered systems considering factors such as maximum energy capacity, scalability, autonomy, and ease of production. The Kite Gen design, labeled KIWI Gen in Lang's presentation, scored the highest overall rating. While each having unique advantages and disadvantages, the five other designs in Lang's report were lacking in either power output or feasibility.

Scoring second was Lang's own design, the Reel mechanism. This small-scale, one-kite design is theoretically simple, but mechanically inefficient in that motors are required to pull the kite back to the start of a cycle decreasing overall net power output. In the reel design, a kite is let out and allowed to rise with a high angle of attack; as the kite rises its turns a reel attached to gears. At the end of this power stroke, the kite is depowered and reeled in by a motor. Other designs included a highly productive but equally unfeasible "ladder" system which relies on a chain of kites cycling up into the atmosphere and back again and turning a flywheel in the same manner as a belt.

This project has also benefited from the work done by an MQP[7] in 2006-2007. The previous year's team researched and analyzed kite power designs before deciding on a conceptual design similar to Dr Goela's, utilizing an rocking arm with a sliding mechanism to change angle of attack. In this conceptual design power is produced by a combination sprag clutch/pump jack which produced power on its up stroke and relied on the weight of the raised beam to return the kite to its original position in the down-stroke. The team also analyzed and tested a number of kites and agreed that a large, airfoil-shaped kite-boarding kite was the best for the application. These decisions and how they have impacted the current project's development will be covered in more detail in the following sections of this report.

In 2008 Olinger and Goela published an ASME report[6] on the preliminary findings from this work. This paper was the first to include a detailed examination of kite aerodynamics in an analysis of a kite power system. Using a Runge-Kutta scheme and assuming a straight line tether, Olinger and Goela numerically solved the governing equations describing how the performance parameters of the system such as output power, cycle time, and tether tension varied with a number of system variables. This work verified the plausibility of a 10 m^2 kite producing 1kW of power at wind speeds below 11m/s.

5 Project Objectives

The goals of this project are as follows:

- Design a prototype of a one kilowatt kite power system capable of harvesting wind energy to produce useful mechanical energy
- Improve prototype existing structure from 2006-2007 project
- Develop an understanding of kite dynamics through field testing for use in autonomous control
- Test structure and subcomponents over a range of expected conditions to ensure stability and safety
- Present results at the 4rth annual National Sustainable Design Exposition for out project sponsor, the US Environmental Protection Agency (EPA)

6 Design Process

6.1 Overall Design

Below is a labeled photograph of our final kite power system (attached to an electrical system designed by separate IQP project).

Figure 6: Final System

The kite power system consists of a commercially available kite-boarding kite and tethers (1), a wooden A-frame, an aluminum rocking arm mounted at a series of pillow blocks (4), an angle of attack mechanism (3), a roll stability mechanism (2), and the power conversion system (5).

The kite (1) is attached to the end of a rocking arm at (2). A roll stability mechanism autonomously ensures that the kite flies in a stable cycle. This mechanism works by rotating the kite's control bar as a reaction to lateral motion. As the rocking arm is lifted up, it in turn pulls a spring loaded rope. The rope turns a shaft and a system of gears and belts with a gear ratio of 6:1 transmit this energy to another shaft. The second shaft attaches to an electrical generator and also contains a flywheel to maintain its motion while on the down-stroke (5). Once the rocking arm has rotated to a given angle, a weight in the angle of attack mechanism slides down, pulling the kite's trailing edge controls and stalling the kite. As the kite stalls and stops producing lift, the arm falls due to gravity and the angle of attack mechanism resets the trailing edge lines to their original tension. The kite again produces lift, restarting the cycle again.

This system has successfully been tested by component and as a whole in a battery of lab and field tests.

6.2 Subcomponent Design

6.2.1 Control of the Kite Lateral Motions

Two kites are used for the project. Both are Peter Lynn kites from a well known manufacturer and supplier of kite boarding kites, with the primary difference between them being the size. The larger kite initially used by the team had a span from wingtip to wingtip of twenty feet with a chord length of five feet. The smaller kite had a span of fifteen feet with a chord length of four feet. Both kites used for the project used a similar control scheme, consisting of a four line setup with two lines attached to the leading edge and two lines attached to the trailing edge. These are attached to a control bar mechanism as shown in Figure 7.

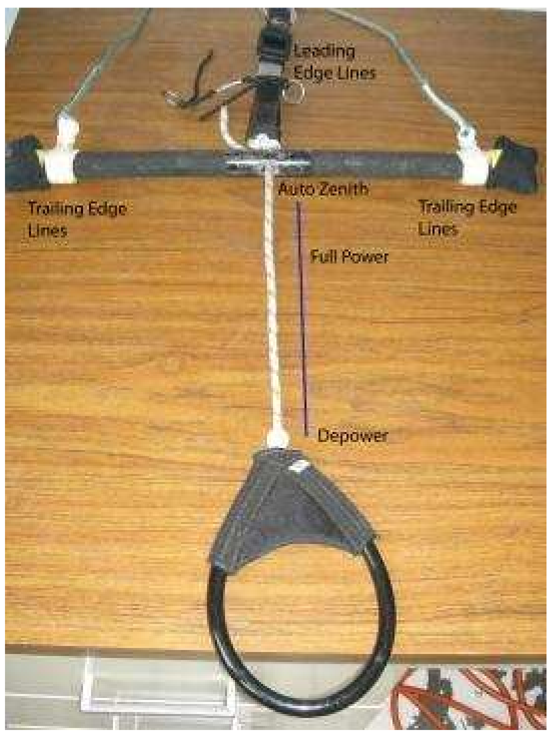

Figure 7: Kite Control Bar

The two center lines are the leading edge lines. These lines experience the highest amount of tension as most of the lift generated by the kite is translated through them to the ring, which for kite boarding would be anchored to the kite boarder. For the kite power system, this line is anchored to the rocking arm. The two outer lines are the trailing edge lines. These lines are under far less tension than the leading edge lines and are the primary means of controlling the kite.

Using the control bar, the kite boarder is able to vary the angle of attack of the kite as well as maneuver its lateral (side-to-side) motion within the power window. The power window is the area in which the kite is able to operate. This is the center 45 degrees of a half-hemisphere volume downwind from the kite anchor point on the rocking arm. Lateral control is achieved by simply rotating the control bar, causing the kite to bank and move in the specified direction. The angle of attack is controlled by moving the control bar in and out while keeping the bar horizontal. Pulling the control bar all the way towards the user, as shown in Figure 7, pulls the trailing edge lines in, increasing the angle of attack so that the kite stalls. At this point the kite is "depowered". As the control bar is moved outward, the angle of attack decreases and the lift generated by the kite increases. The kite is fully powered, generated the maximum amount of lift, when the control bar is approximately three quarters of the way out, which can be seen in Figure 7. Moving the control bar beyond this point is referred to as "auto-zenithing." In this mode, the kite has very little pull and flies almost directly overhead with little or no user input.

In order to achieve the goal of autonomous power generation, a mechanism had to be designed to control the lateral motion of the kite. With no control input, disturbances such as wind gusts can cause the kite to move to the side, as shown in Figure 8.

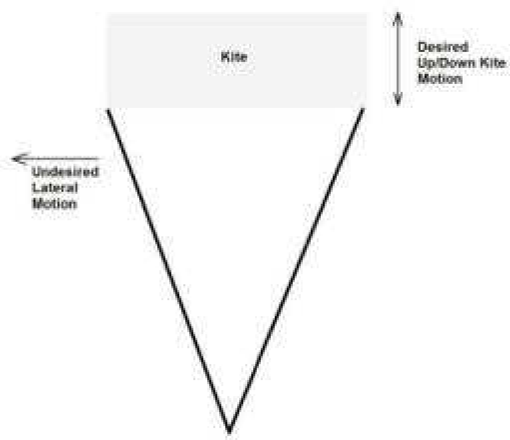

Figure 8: Kite Motion

Uncorrected, this behavior often results in the kite crashing. After a largely evolutionary design process, we arrived at the design shown in Figure 9. The basic premise of this design was to apply a rolling control input in the opposite direction of the kite motion. The pivoting center arm would be able to move from side to side as the kite moved to either direction. As it does this, the side control arms would hold the control bar, in effect rotating it with respect to the kite. This causes the kite to move back towards the center of the window. The angle of attack slide allows the entire mechanism to be moved in and out to allow for lateral control at all angles of attack. Field testing showed that this design was able to satisfactorily control the lateral motion of the kite in reasonable wind conditions, allowing it to remain in the air indefinitely. Field testing will be further discussed later.

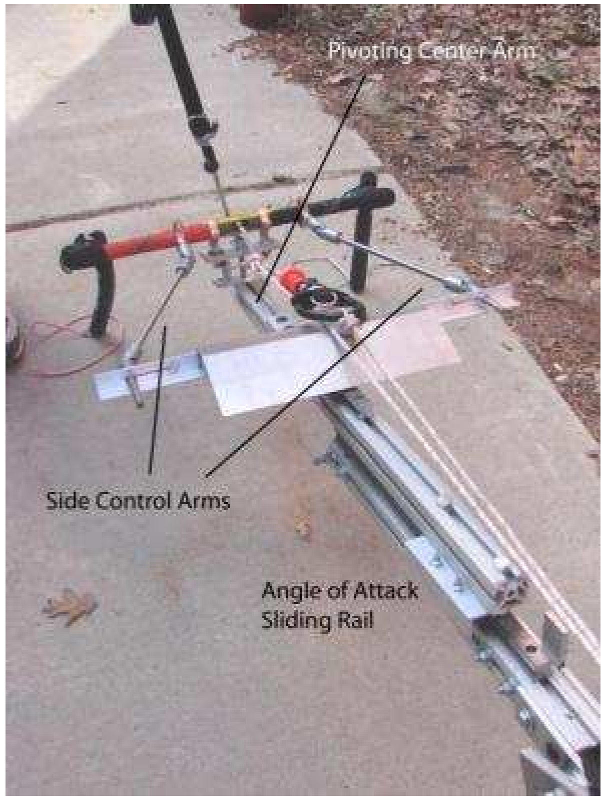

Figure 9: Kite Control Mechanism

Initial designs focused on the use of springs to dampen the lateral motion of the kite. Two springs would be attached to the control bar, one to each end. Lateral motion of the kite would cause the control bar to rotate. As the bar rotated, one spring would be put into tension while the other was put into compression which would create a force in opposition to the rotation of the control bar. A conceptual sketch of the mechanism is shown in Figure 10.

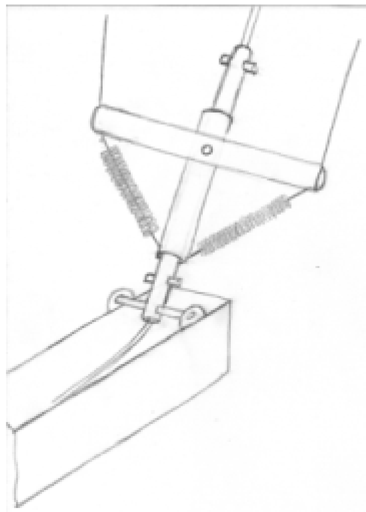

Figure 10: Conceptual Sketch of First Kite Control Mechanism Design

A sliding mechanism was incorporated into this design in order to allow for angle of attack control. The springs were attached to the sliding part so that they would slide with the bar, keeping the tension constant at all angles of attack. This design was tested on several occasions, with modifications made between each testing session. Initial modifications centered on strengthening the mechanism to allow it to withstand the high forces exerted by the kite. Changes were also made to allow the control bar to slide more freely. Figure 11 shows a later design of the spring concept.

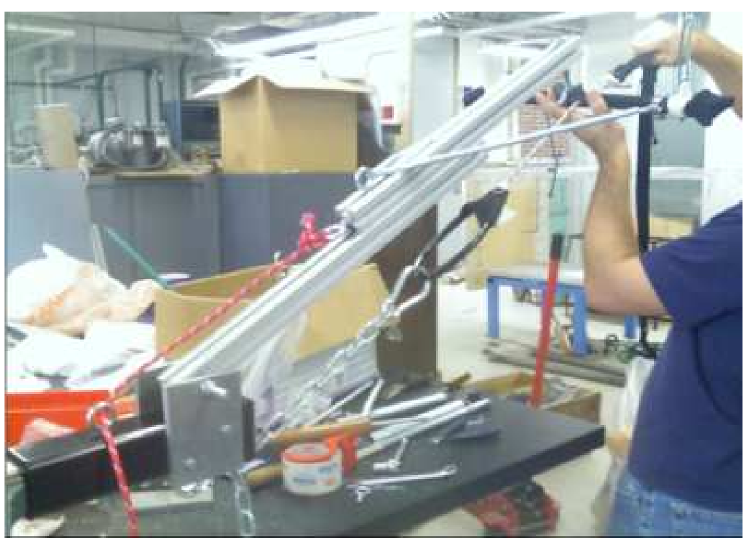

Figure 11: Strengthened Spring Control Mechanism

A variety of spring sizes were used in effort to adequately control the kite motion. After several unsuccessful tests, it was decided that the dampening effect of the springs was insufficient to counter the lateral motion of the kite.

A new design was needed and based off the previous testing experience, it was decided that the control mechanism had to be able to turn the control bar to oppose the motion of the kite. A conceptual design is shown in Figure 12. The constructed version of this design is shown in Figure 13, which is the control mechanism used for power generation.

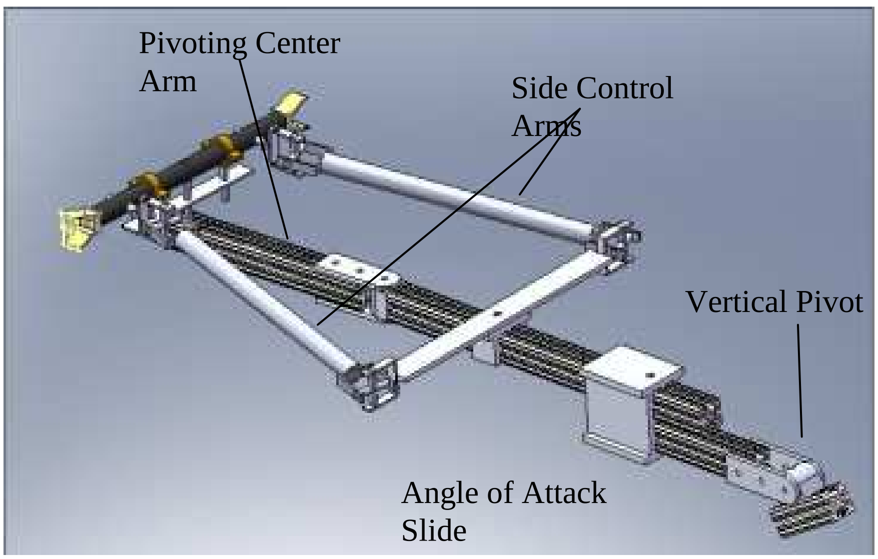

Figure 12: Design of New Concept for Kite Control Mechanism

Figure 13: New Kite Control Mechanism as Built

Any lateral motion of the kite would pull the control bar and the center pivot in the same direction. The two shafts attached to either side of the control bar force the control bar to rotate in the opposite direction, exerting a force on the kite to bring it back to center. Video showing the operation of this mechanism during field testing in Rhode Island can be found on Youtube[13].

Field testing showed that this design was capable of controlling the lateral motion of the kite. Initial testing was done with the control mechanism anchored to the trailer hitch on a pickup truck. Occasional user input was still required to handle drastic kite motion. However, for reasonably small perturbations, the mechanism was able to control the lateral motion of the kite, keeping it in the power window. Several modifications were made to improve the design. A new bearing was added to the sliding mechanism which was better able to handle the high off-center loads applied by the kite. The pivot which allows the mechanism to rotate vertically as the kite powers and depowers was strengthened, again to better withstand the off center forces.

With these modifications, the kite could be flown for extended periods of time with almost no human intervention required for lateral control. The only user input required was to control the angle of attack, which was made significantly easier by the new bearing. Once the design had proved itself under those conditions it was attached to the rocking arm of the kite power system. Figure 14 shows the control mechanism attached to the rocking arm.

Figure 14: Kite Control Mechanism Attached to Rocking Arm

This setup was tested and shown to be able to handle to large forces exerted by the kite. With this final step completed, the team had a mechanism in place which was capable of controlling the lateral motion of the kite while allowing for the angle of attack to be changed in order to create the power/depower cycle necessary to create electricity.

6.2.2 Angle of Attack

The reason that the kite can generate power is its cyclical action between a powered and a depowered mode. This behavior is caused by changing the angle of attack (AOA) of the kite which powers the kite at lower AOAs and stalls it at higher AOAs. Consequently, the mechanism which changes the AOA is crucial to the functioning of the entire system.

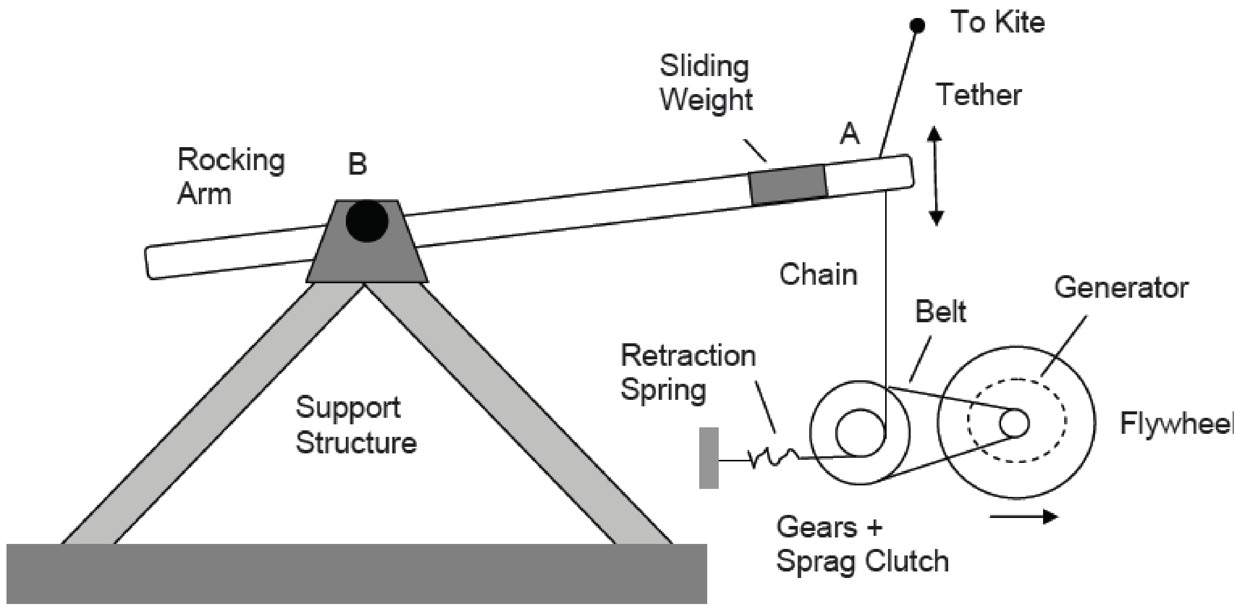

Figure 15: Rocking arm diagram[6]

There are two control lines attached to the leading edge of the kite and two attached to the trailing edge. When the arm is in the position shown in Figure 15, the weight, which is attached to the rear control lines, rolls towards point B. This increases the AOA, pulls on the trailing edge lines, and stalls the kite to decrease lift. When the retraction spring pulls the arm back down, the weight rolls back to A and the trailing edge lines are released, which decreases the AOA and increases the lift on the kite. The arm then rises again and the cycle repeats, causing the rocking motion of the arm to be converted to electrical energy.

Since it is very difficult to predict the required weight, length of motion, and timing of the rolling weight, it was necessary to develop a flexible design where those three properties could be varied. To deal with the issue of exactly when the weight should start rolling to change the AOA, we designed a system where the weight, before moving, would have to roll past a tensioned gate. For this we used spring hinges frequently found on two-way screen doors. There is one gate on both ends of the weight's track to control the start time of descent for the power and depower cycle. In addition, the hinges have tension control which we can use to fine tune the timing of the weight. The weight rolls on two trolleys which fit into strut channels and the amount of weight can easily be changed. Lab testing was conducted on the mechanism to determine angles at which the rolling weight overcomes the tension in the hinge. Figure 17 shows the results.

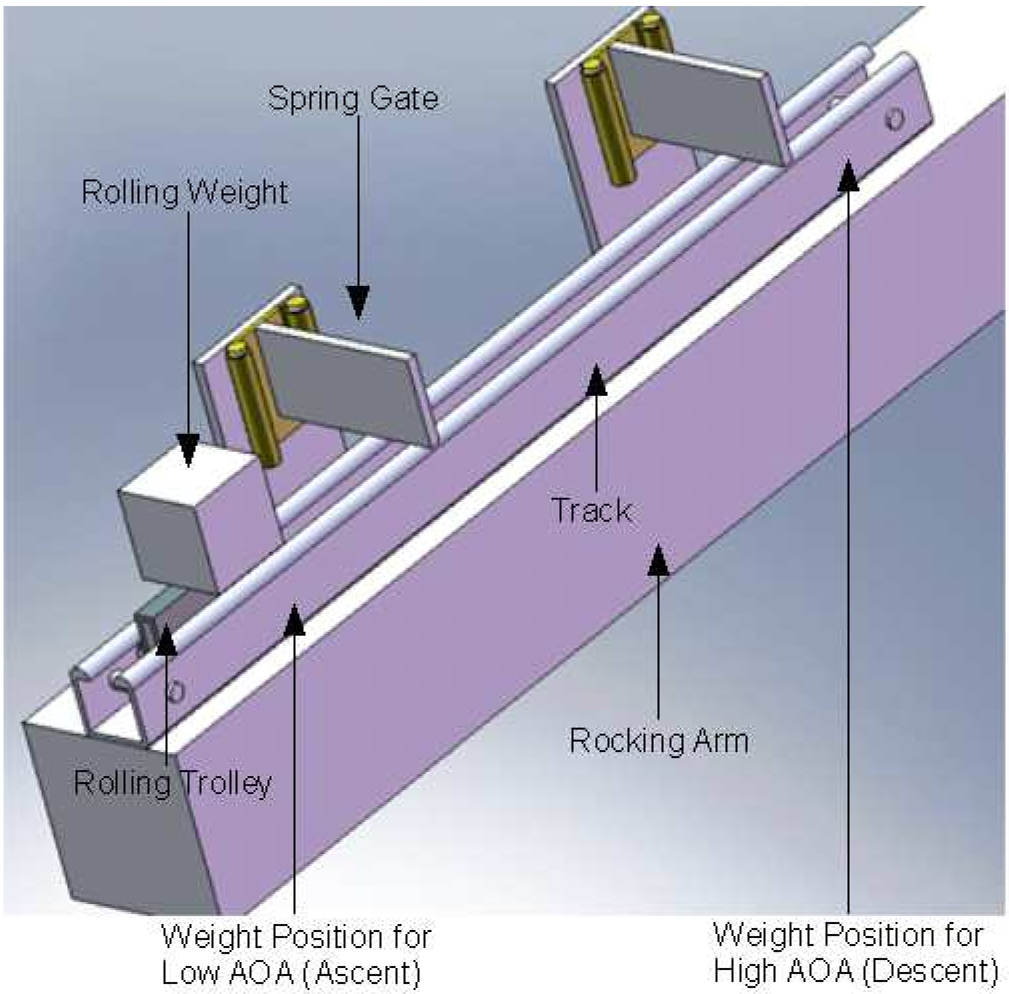

Figure 16: AOA change mechanism

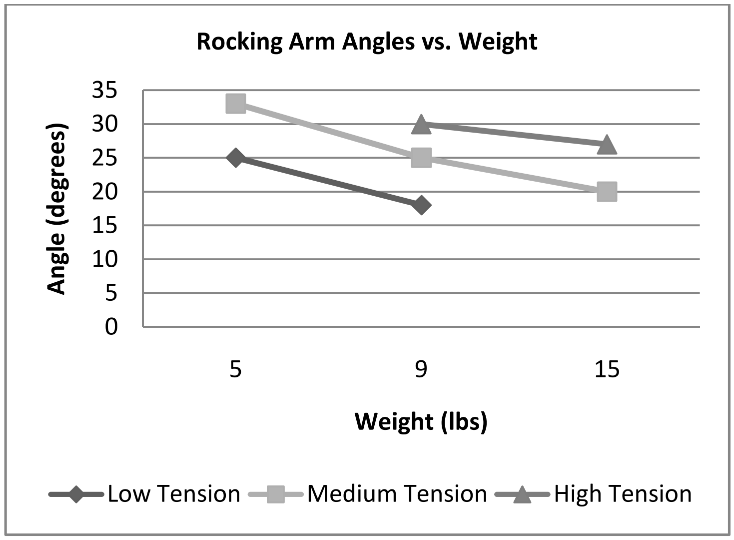

Figure 17: Rocking arm angles vs. weight

6.2.3 Power Conversion System

The power conversion system is responsible for converting the linear motion of the arm into rotational motion, then transferring that rotational motion to a generator. The system also contains a flywheel to store mechanical energy, which allows the system to stay spinning when the rocking arm is on its down stroke. Lastly the power conversion mechanism utilizes a retraction spring to rewind the tether that links the beam to the power conversion system.

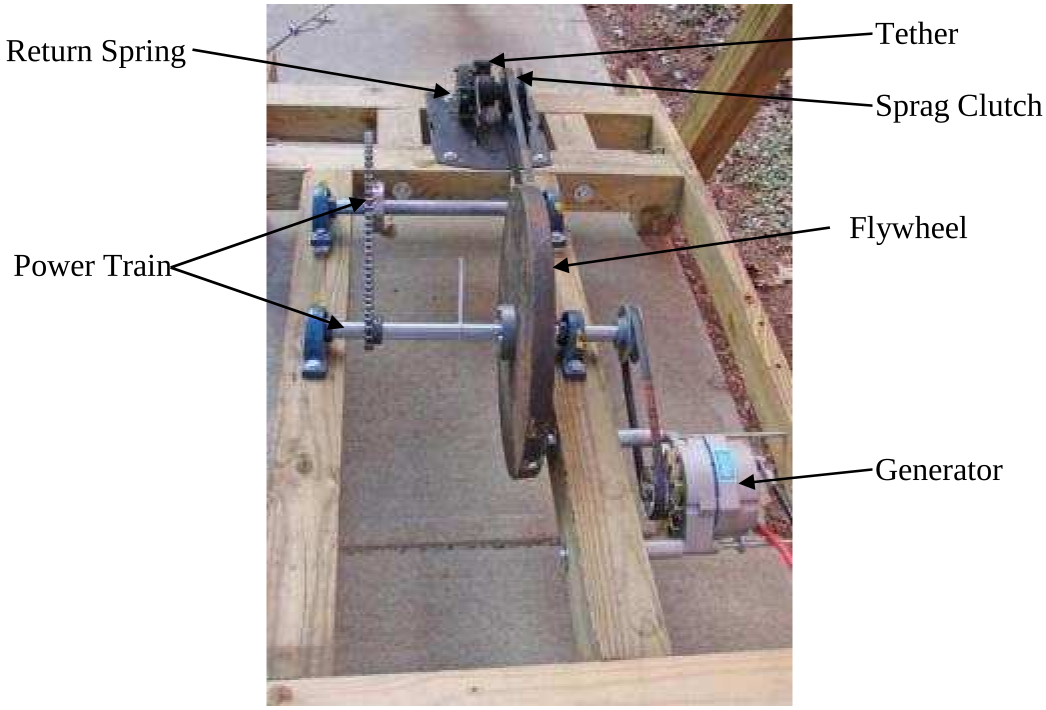

Figure 18: Diagram of power conversion system

6.2.3.1 Sprag Clutch

As mentioned previously, the system goes through two stages while generating power, the power stage and the freewheel stage. To allow for the system to generate rotation in one direction and have no influence in the other direction a sprag clutch is used. The sprag clutch used in the system was adapted from a rowing machine and resembles a ball bearing. However, it differs from a ball bearing in that it spins in only one direction and is inhibited from spinning in the other. This allows the tether to be pulled, in turn rotating the first shaft in the power conversion system on the up stoke, and spin without influence from the tether on the downstroke. When the aforementioned retraction spring pulls in the tether and this same shafts reverses direction in order to wind it up, the sprag clutch disengages allowing the remainder of the power conversion system to be unaffected.

6.2.3.2 Power Train

In order to transfer the rotational motion to the generator, a power train was developed. Also the power train was designed to provide a final gear ratio of approximately .6:1. This "gearing up" allowed the final shaft that would be connected to the generator to be spinning at a much higher RPM, approx 1200, than the shaft with the tether attached to it. This was necessary to get adequate voltage from the generator.

6.2.3.3 Flywheel

This system depends on the switching between power and freewheel cycles, which could lead to times where the power conversion system would be spinning at high speed and then not at all. What was desired was to have the system continue to spin while in the freewheel stage. This is desirable because when the system spins at a constant rate the power output from the generator will also be constant. When this system is spun normally the resistance from the generator and the natural friction of the system causes it to stop spinning immediately after the beam stops influencing the power conversion mechanism. In order to get a more constant spin a flywheel was added into the power train. The flywheel is basically a large metal disc with a high rotational moment of inertia, which means once it starts spinning it will resist the frictional forces and keep spinning. Two flywheels were used during testing. Their specifications are included in Table 1.

Mass	20.4 kg	11.3 kg
Diameter	44 cm	26.9 cm
Moment of Inertia	0.483 kg m^2	0.103 kg m^2

Table 1: Flywheel Specifications

Moment of inertia was calculated using the thin disc assumption where, $I = \frac{1}{2}MR^2$. M is the mass of the disc and R is the radius.

The down side of a flywheel is that while it will spin for longer, it takes a lot of force to get it spinning in the first place. This resistance to spinning makes it difficult for the system to get the flywheel up to operating speed, and it usually takes 2-3 power cycles to achieve this.

6.2.4 Kite Bouyancy

An important technical hurdle to overcome is the issue of a no-wind condition. Although large kites can fly in very low wind speeds, and higher altitude winds are much more persistent and strong than ground-level winds, there is still the possibility of a complete loss of wind, in which case the kite would fall to the ground. This presents several issues, including the necessary re-launching of the kite, as well as possible impacts on objects below. To solve this problem, our team investigated the use of helium to buoy the kites in case of a loss of wind.

Because our kites are twin-membrane, with a hollow interior, it is possible to insert helium bladders into the individual cells of the kite. To this end, we created openings in the trailing edge of 11 cells on our 10 sq. meter kite and sewed Velcro strips into the trailing edge in order to seal these openings during flight. This allows for access into these cells, where the helium filled bladders or balloons can be inserted. The usable volume of these cells was computed, and then experimentally confirmed, to effectively allow for the helium bladders to loft approx. half of the kite's weight. Although this does not make the kites completely buoyant, it will allow for the kite to fly in lower speeds due to the decrease in lifting force necessary to loft the kite's weight.

In order to make the kite completely buoyant, rip stop nylon sleeves were sewn to accommodate the remaining necessary helium external to the kite. These sleeves are roughly 5 feet long, with a diameter of approximately 3 feet. They will be attached at the wing tips of the kite, between the leading and trailing edge control lines. Filling these sleeves with helium bladders will account for the remaining buoyancy required to lift the kite.

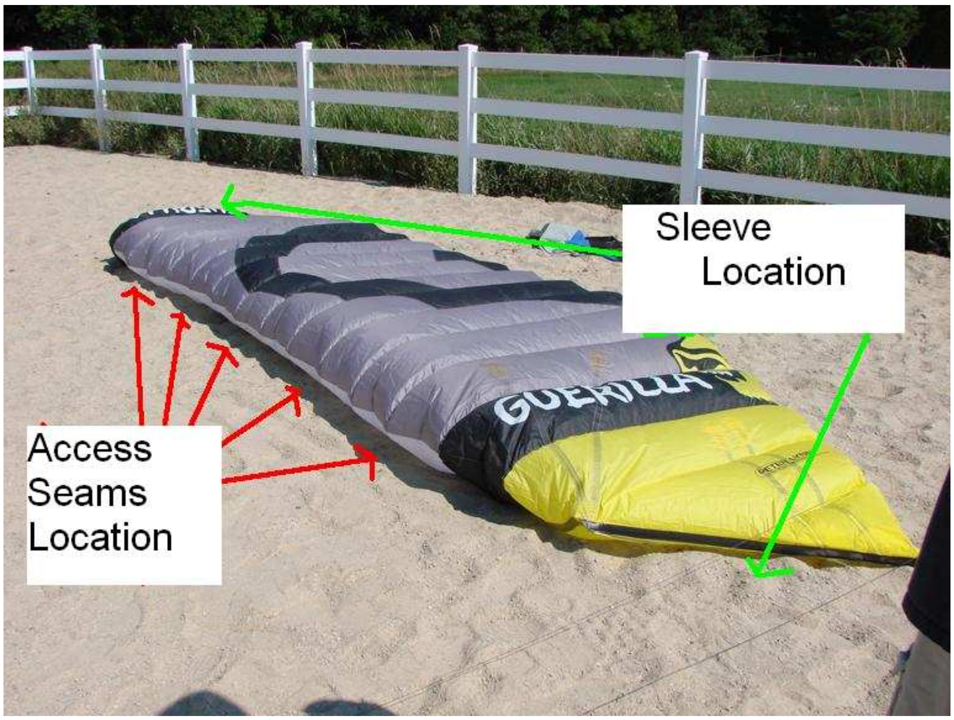

Figure 19: Kite with buoyancy locations

In the future, this solution to the kite buoyancy issue will need to be further addressed in several areas. First, the flight dynamics of the kite with the helium bladders will need to be assessed through flight testing, as well as using the kite simulation developed by Olinger and Goela (2008). The main issues will be the increase in drag associated with the internal bladders and external sleeves, as well as the effect of a buoyant force on the dynamic equations of motion. Additionally, it will have to be determined whether or not the kite will still be able to crash, even if it is effectively weightless. Also, the helium bladders add a significant amount of weight to the kite, meaning more helium is required. A possible solution is to use a helium-tight kite, which introduces added cost and complexity.   In conclusion, a helium-lofted kite does seem to be the most simple and effective way of preventing the kite from falling due to a loss of wind, but a continuation of our team's analysis will be needed to determine the most effective method of implementation.

6.2.5 Structural Improvement

The structure for the power generation mechanism is an A-frame structure which supports the aluminum rocking arm. The original structure built by the 2006-2007 MQP team is shown in Figure 20 below. Initially, the arm was mounted to the top cross-beam of the base structure by two pillow block bearings attached to the steel sleeve which supports the center piece of the aluminum arm. These pillow blocks shared a common shaft with two other pillow block bearings mounted on the wooden cross-beam, and it was around this shaft which the entire arm rotated.

Figure 20: Original mechanism

However, this construction presented two major problems. First, the considerable length of the aluminum arm meant that any sideways force at the end of the arm subjected the pivot point to significant moments about the vertical axis. These moments proved too large for the pillow blocks mounted on the wooden cross-beam as the bearings were beginning to wiggle their bolts loose. Consequently, the arm would experience significant yaw for even relatively small sideways forces applied to the ends of the arm. Second, the large moments were also inducing high magnitudes of stress in the wooden structure, especially at the intersection of the wooden cross-beam and the legs of the structure. Our goal was to eliminate the yaw of the arm, and better allow the structure to handle the large moments developed by the sideways forces that will be applied to the arm when the mechanism is in use.

Our first step was to widen the stance of the pivot of rotation at the center of the arm, in order to reduce the torques that each pillow block experiences. To do this we added a ¼ inch steel plate between the steel sleeve and its two pillow block bearings. The plate is 36 inches long, which allowed us to install pillow block bearings onto the bottom of the plate 15 inches from the center on each side. We also installed two additional pillow blocks onto the wooden cross beam 12 inches outward from the two central bearings. We replaced the original shaft with

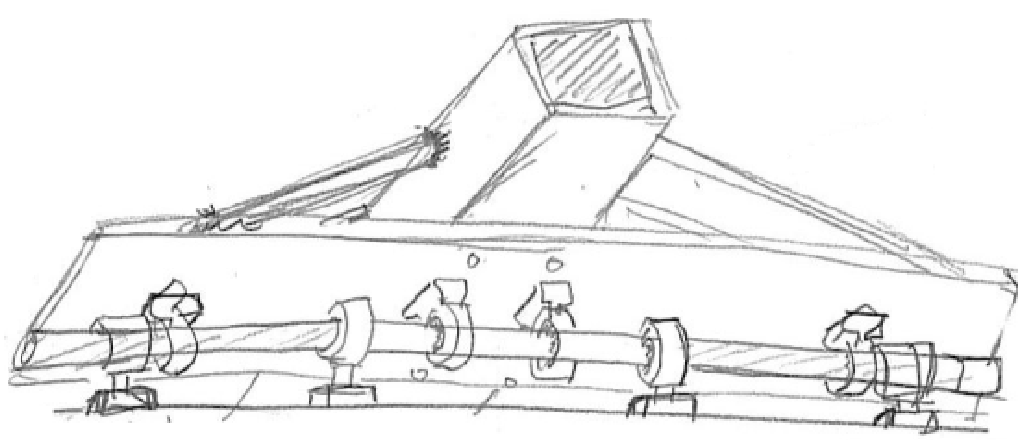

Figure 21: Structural Redesign of the Pivot Point

a new 4 foot shaft which all eight pillow block bearings now share (Figure 21).

Additionally, we bolted four struts diagonally from the plate to the arm itself to further brace the arm against yaw. The struts were made from ¾ inch aluminum conduit tubing. The installed plate and struts are shown here.

Figure 22: Structural Improvements

Bracing of the wooden structure involved installing metal angle brackets onto the weakest corners of the structure, and anchors at the base of the legs to hold the structure to the ground during operation.

A rigorous stress analysis was later conducted to test these improvements.

6.2.6 Safety Precautions

Considering the magnitude of the kite forces (approximately 200 lbf tether tension) created in the kite power system, safety was one of the most important aspects for the team to look at. Several precautions were taken, not only to prevent an accident from occuring, but to also to curb injury in unexpected incidents. In addition to always maintaining awareness and ensuring proper communication when working on the system and its components, the project team implemented the following safety precautions.

6.2.6.1 Lock out Mechanism

The safety team designed a lock out mechanism for the rocking arm. The purpose of this mechanism was to hold the arm in a horizontal position, which allowed the team to work on the structure without the difficulties and danger of a large freely rotating arm. The final design (Figure 23) consists of sheet metal secured with two pieces of 3/8” rod. Figure 24 shows this mechanism in place, holding the beam horizontal. Because the brunt of the loading due to the weight of the beam is actually taken by the two pieces of rod, simple sheet metal is sufficient. The rods transfer the load to one of the main structural supports, which is capable of handling the load. The lock out mechanism proved very useful during winter testing indoors as it allowed the project team to safely lay the structure on its side and test lateral loading on the beam, without having to diassemble the entire structure. It was also used to aid in transporting the sturucture. With the lock out mechanism in place, the center portion of the beam did not need to be dissassembled during transportation.

Figure 23: Lock Out Mechanism

Figure 24: Lock Out Mechanism in Place

6.2.6.2 Hard Hats/Safety Padding

To prevent serious head injury from the weight of the rotating beam, the team took two main actions; hardhats and padding. Hard hats were required to be worn by anyone in the vicinity of the structure. This procedure was important not only while working on the beam, but also during testing of other components throughout the duration of the project. To further soften the impact of the beam striking anything, the team chose to line the bottom with ahigh density HVAC duct lining Figure 25. This padding was an ideal choice mainly because of its high density, which allows maximum distortion and energy absorption. The padding was originally fastened to the beam using hose clamps. However, due to the difficulty of installing and

Figure 25: HVAC Duct Lining

removing the hose clamps, a design change was implemented in which nylon straps with velcro replaced the hose clamps.

To test the effectivness of the hard hats and padding, a "Cantaloupe Test" was conducted. This test consisted of dropping the beam from a raised position onto a cantaloupe direcetly underneath the beam. The setup of the test can be seen in Figure 26. The cantaloupe was placed on small table to simulate someone crouching, possible working on a piece of the structure. Two cases were tested. The first consisted of dropping the beam with no padding of the bottom onto a bare cantaloupe; the second with the HVAC liner and a cantoloupe with a hard hat. Figure 27 demonstrates the comparison between the outcomes of the two cases, with the first test on the left and the second on the right. As one can see from the pictures, the beam completely smashes the first cantoloupe, while the second cantaloupe remains intact. These experiments gave the project team reassurance in the effictiveness of the hard hats and padding, as well as a good example of why hard hats always need to be worn.

Figure 26: Setup of Cantaloupe Test

Figure 27: Outcome of Cantaloupe Test

6.2.6.3 Release Mechanism

Another area the safety team needed to look at was the design of a mechanism that would allow for remote release of the rotating arm while the kite was attached. This was especially important for early tests with the kite attached. Because the team anticipated the kite would be in the powered region and have a fair amount of pull, the arm needed to be secured in the lowered position while the kite was being attached. For this reason, it is best to have everyone clear of the arm when it was released. The release mechanism designed for this problem Figure 28 consists of a short piece of chain, a 3/8" latch pin, and a metal bracket. One end of the chain is attached to a brace on the bottom of the structure and the other is attached to the arm via the metal bracket and latch pin. The latch pin has a 6 ft. long piece of rope which allows it to be pulled out, releasing the arm from a distance and allowing for a safe remote operation.

Figure 28: Release Mechanism

7 Testing Methodology

Before field testing of the entire kite power system could be considered, each component was lab tested to determine its performance under load. The first series of tests were static, meaning forces applied did not change over time. Static tests were followed by dynamic tests. Dynamic tests were involved to verify the beam and structure's ability to endure short to mid-term cyclical testing in conjunction with the kite during future development. The sections to follow describe, in more detail, the test setups and the results obtained after completing those tests.

7.1 Static Test Setup

As summarized previously, the function of the static tests is to verify the arm's performance and structural rigidity under load. For this test the rocking arm was fixed in a horizontal position with one end chained down to the structure. On the opposite end a metal basket was attached to the beam using chain and an eye bolt inserted through a previously drilled hole in the beam. Weight of the basket and accessories summed to approximately 200 lb. Figure 29 shows a sketch of a side view of the test setup.

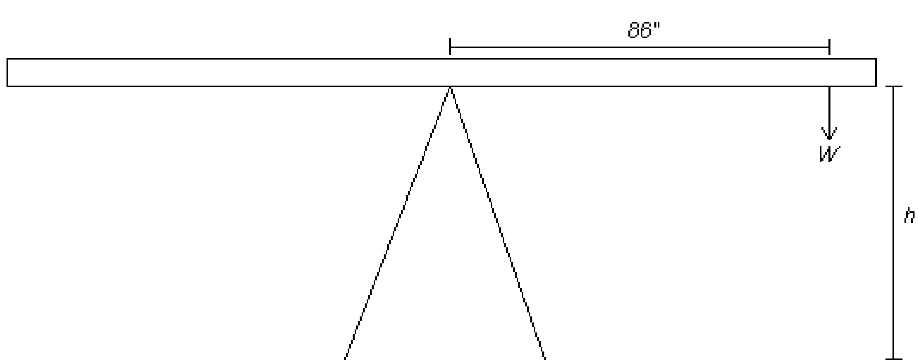

Figure 29: Vertical Test Setup

Once the setup was complete, initial measurements of the beam end height were taken. Next, weight was added to the basket incrementally (see Figure 30). Once the arm was loaded, a measurement of the arm's deflection was taken.

Figure 30: The Beam Weighted Down

A second static test was conducted to observe what would happen to the structure given a high loading in the lateral direction, i.e. perpendicular to the previous test. To do this the structure was tipped on its side, similar to Figure 34.

7.2 Static Test Results

The beam loading test results can be seen below in Figure 31 and Figure 32. As you can see, the deflection from the beam did not exceed 2.5 inches, even under a loading of over 150 lbf. Based on the length of the rocking arm, these deflections were acceptable.

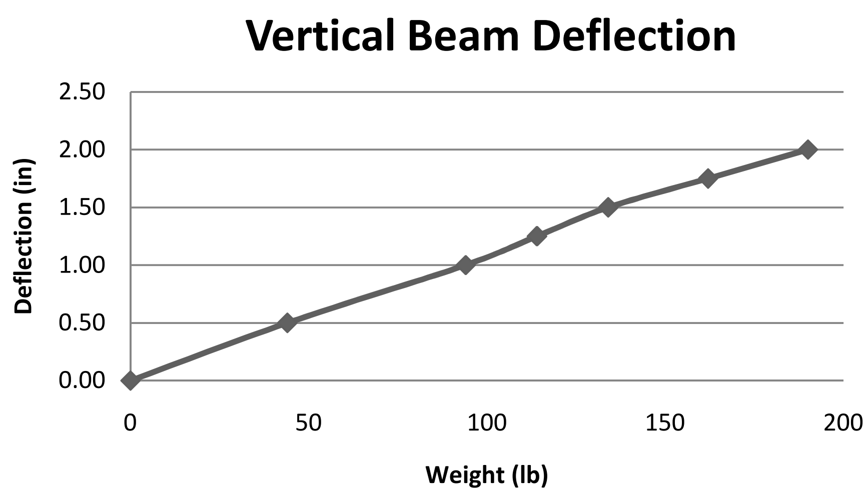

Figure 31: Vertical Loading, Weight vs. Deflection

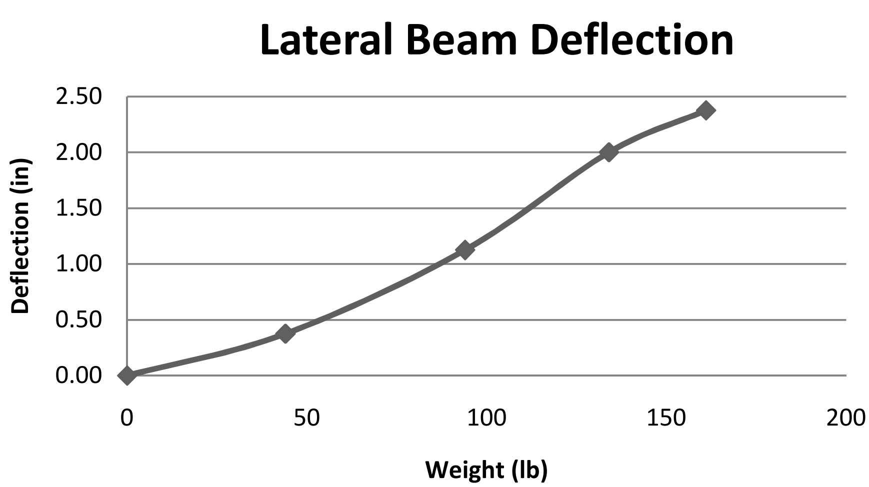

Figure 32: Lateral Weight vs. Deflection

7.3 *Dynamic Test Setup*

In order to simulate the potential wear and tear the kite and its motion will have on the structure, dynamic testing was a combination of two setups. First a rope was attached to the beam end where the kite is planned to be attached. That rope was then routed through a pulley on the ceiling so that the beam could be lifted up and down via the rope while the operator stood at a safe distance. The critical part of the test was cycling the beam up and down, allowing it to free fall into a pile of used tires, Figure 33.

Figure 33: Free Fall into Tire Pile

The test was continued through 1000 cycles with time taken to observe the beam and structure at about every 100 cycles.

The second setup involved turning the structure on its side. A rope, identical to the one mentioned previously, was attached to the beam end at approximately the location where the kite will attach. Next a loop (or bight) was tied into the rope so that a spring and weight system could be implemented (Figure 34).

Figure 34: Dynamic Test Setup

The spring that was used is a large garage door spring, rated to lift a 175lb door. Approximately 82 lbs was attached to the spring and then set into oscillation by displacing the weight such that it would cycle with an amplitude of 18 inches. This effectively simulates cyclical side forces that mimic those the kite will apply as it flies across the sky. The amplitude of the loading was calculated and can be seen in Figure 35 below. The test was conducted through a few cycles, with careful observation taken during and post test.

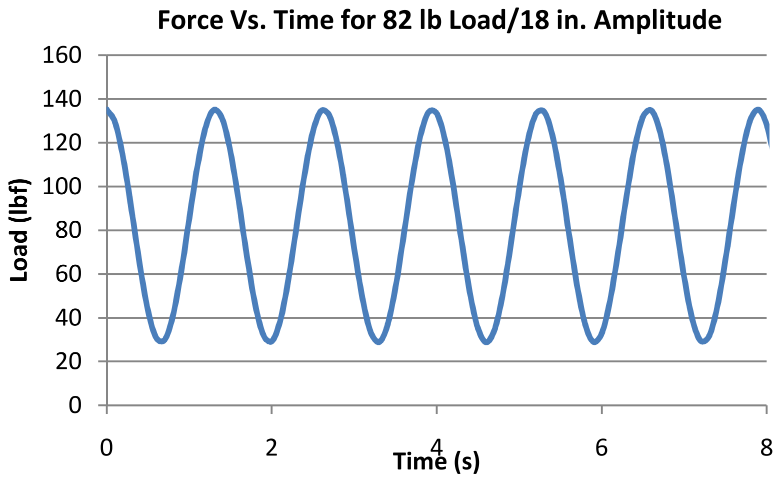

Figure 35: Loading Over Time

In order to get a benchmark for a worst case scenario, the test above was done without the spring. This creates an impact loading that creates a large force over a short time; effectively simulating the kite rapidly changing direction. Given the limitations of those conducting the experiment, the amount of weight was set at 50 pounds and was dropped from approximately two feet. Based on the deflection of the beam, the drop was estimated to be the equivalent of a 175 pound side load, applied over a period of about .25 seconds. Deflection was estimated by observing a tape measure placed next to the beam during the test.

7.4 Dynamic Test Results

The data taken from the dynamic tests was made up entirely of observations of the structure, the beam, and all of the points of attachment. It can be generalized that the structure showed little to no damage after both cycle tests and should hold up well during long term use. While the effects of weathering on durability could not be directly determined from these tests, it would most certainly decrease the lifespan of the structure. Even during the drop test, the maximum deflection was only approximately two inches.

8 Field Testing

In addition to our laboratory testing, which was mainly conducted to evaluate the structural strength of our mechanisms, field testing was conducted to determine their real world performance. The majority of our testing took place at a public beach in Seabrook, NH, due its consistent wind conditions, and Mesa Farm in Rutland, MA, nearby to Overlook Farm. The tests dates were heavily influenced by the weather, as most of our testing fell during the winter months in New England. We were able to test on days when the weather co-operated, especially the wind conditions. We determined the approximate wind speeds in advance using NOAA's website[14], which gives accurate predictions of wind velocity and direction several days in advance.

The majority of our testing was devoted to developing and refining the kite control mechanism, as this presented the most pressing technical challenge of our project. The initial design, two springs configured on either sides of the control bar, was tested two times in A term 2007. The initial test, conducted at Mesa Farm, was unsuccessful, so the team decided to test again using springs of different force constants. When the second test once again proved unsuccessful, the team realized a new design was necessary. Our experience in these tests, as well as our observations of the basic fundamentals of kite control, helped us to realize that the kite control mechanism needed a complete re-design. This design can be seen in more detail in the roll stability subcomponent section.

Our first field test of the second design resulted in a near-immediate failure of a bolt holding the device to the truck hitch that the kite was anchored to; another example of the considerable force the kite is capable of generating. Upon inspection, we found we had attached the kite leading edge tether lines improperly to a bolt on the control mechanism as opposed to the truck hitch. As a result, this small bolt took the entire kite load.

This failure had two results: the control mechanism was significantly strengthened to handle larger forces, and our safety procedures were increased. After this, we always ensured that the leading edge lines were attached to the truck hitch or to the end of the rocking arm in later test. In our later field tests, chest and head protection were also worn by students operating the kite control mechanism to prevent injuries in case another failure occurred. Over the remainder of B and C terms, the control mechanism was tested several more times. These tests showed conclusively that the design was adequate to control the kite, as demonstrated by the videos taken on our testing days. A picture of the control mechanism being tested is shown in Figure 36.

Figure 36: Roll stability test[15]

After determining that the kite control mechanism design was viable, we needed to make sure the structure would not tip over while the system was in operation. To this end, four anchors were attached to the A-frame structure and planted in the beach at Seabrook. A rope was then attached to the end of the arm at the point where the kite exerts force. Four members of the team pulled on the rope to simulate several hundred pounds of side force exerted by the kite, significantly more than the kite will generate. After repeating this test several times without the structure tipping, we determined that the anchors would be sufficient to stabilize the structure while in operation.

With the structure having passed all its structural tests, and with the team being confident that the control mechanism could successfully control the kite, the next step was to fly the kite, attached to the rocking arm which was fixed, by attaching the arm to an anchor. This test was conducted at Mesa Farm on March 26, 2008 in approximately 13 knot winds. The kite flew for over a minute and completed several power cycles, without failure in the structure or control system, as shown in Figure 37.

Figure 37: Kite flying on fixed arm[16]

This led to our last, and most exciting test which was generating power for the first time. This test was conducted at Seabrook, NH on April 6, 2008 in approximately 18 knot ground level winds. Once again, the rocking arm was fixed to the ground, but this time approx. 1-2 feet of arm stroke was allowed so the generator could be turned. The kite successfully completed several power cycles and turned the power conversion mechanism and generator shaft. Since the arm stroke was very limited, only a small percentage of the system's potential power was generated. However, the system did produce measurable power over several minutes, thus proving that our kite power system is feasible and capable of extracting power from the wind. In the near future, tests allowing a greater arm stroke will be conducted, culminating in a full-scale test, which will allow us to see the full power potential of the system.

Figure 38: First power generated[17]

9 MATLAB Dynamic Simulations

The project team utilized a MATLAB simulation developed by Dr. David Olinger and Dr. Jitendra Goela. The theoretical basis for the model is derived from the previously mentioned work done by Dr. Geola. The work done by Dr. Goela was modified to more accurately represent the kite power system developed by the project team by including the power conversion system, which requires incorportation of the gearing and flywheel into the dynamics of the simulation. A brief overview of the governing equations for the model will be given here. A detailed derivation is available in Olinger & Goela[6].

Before introducing the main governing ODEs for the simulation, the following variables must be defined:

F_{DK}	= drag force on kite
F_{LK}	= lift force on kite
F_t	= tether tension
g	= gravitational acceleration
I_{AD}	= moment of inertia of rocking arm
I_F	= moment of inertia of flywheel
K	= retraction spring constant
L_t	= tether length
M_{AC}	= moment about aerodynamic center of kite
R_A	= half-length of rocking arm from B - A
R_C	= radius from pivot B to chain attachment point
R_{CTR}	= radius of counter weight
R_F	= radius of flywheel
R_{FG}	= radius of gear FG
R_G	= radius of gear G
R_{G2}	= radius of gear G
V_A	= velocity of end of rotating arm (point A)
V_{2A}	= velocity of kite normal to tether w.r.t. point A
W_{BA}	= weight of rotating arm: pivot B to point A
W_{CTR}	= weight of counter weight
W_{DB}	= weight of rotating arm pivot B to point D
W_F	= weight of flywheel
W_K	= weight of kite
W_{LOAD}	= weight of load
Δx	= retraction spring deflection
γ	= angle of rotating arm
θ	= angle of kite tether with respect to horizontal
ϕ	= angle of local velocity vector V_R w.r.t. ground
ω	= angular velocity of rotating arm
$\Delta z_{LOAD2-4}$	= elevation change of load weight : engaged
$\Delta z_{LOAD4-2}$	= elevation change of load weight: disengaged

The model is based on energy conservation throughout the individual components of the kite power system. A general visualization of the the way the model works is shown below in Figure 39, adapted from Olinger & Goela[6]. When the arm is pulled up by the kite, the clutch and flywheel are engaged and accelerate as the arm moves up. A load is also attached to the system and the load raises as the the flywheel rotates. When the arm is on its downstroke, the clutch and flywheel are disengaged from the arm. However, the flywheel continues to rotate and raise the load. Power output is measured by calculating the overall increase in height of the weight for each cycle. Other outputs from the simulation include arm angles, tether angles, tether forces, flywheel speeds and flight path of the kite.

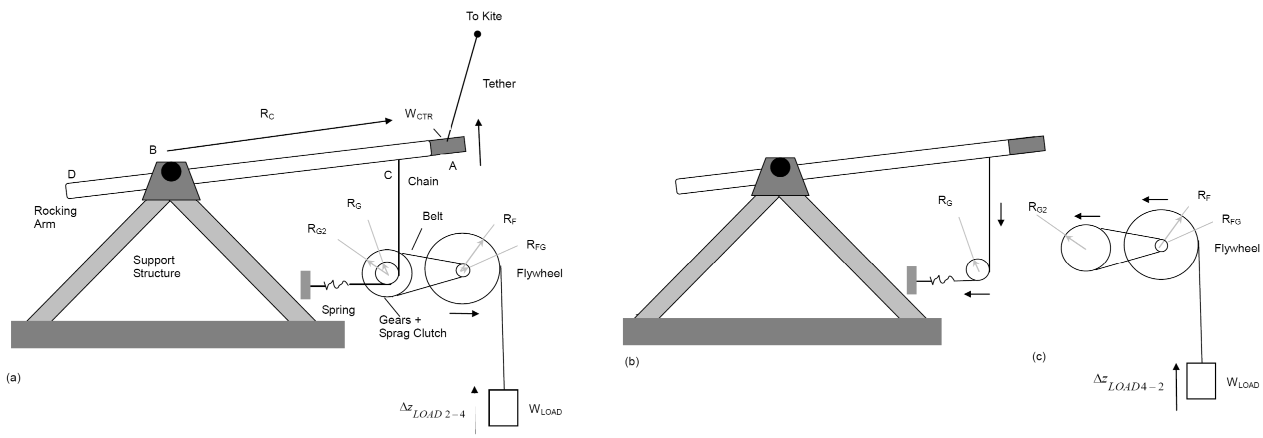

Figure 39: Visualization of MATLAB Simulation[6]

The five governing ODEs for the model are shown below. Equation 2 relates the acceleration of the end point of the arm to the forces acting upon it. Equation 3 relates the acceleration of the kite in the direction normal to the tether to the forces acting upon the kite. Equation 4 shows that the energy that is put in or taken away from the flywheel goes into raising the load. Equation 5 and Equation 6 describe how the change in angle of the kite tether and rocking arm is related to the normal velocity of the kite and velocity of the end of the arm, respectively.

$$\frac{dV_A}{dt} = A\begin{bmatrix} F_t R_A \cos(\gamma - \theta + \pi/2) - W_{LOAD}\dfrac{R_{G2}}{R_{FG}}\dfrac{R_F}{R_G}R_C \\ - K\Delta x R_C - M_{AC} \quad - W_{BA}\dfrac{R_A}{2}\cos(\gamma) \\ + W_{DB}\dfrac{R_D}{2}\cos(\gamma) + W_{CTR}R_{CTR}\cos(\gamma) \end{bmatrix} \tag{2}$$

where $$A = \frac{-1}{\left[\dfrac{1}{g}\dfrac{I_{AD}g}{R_A} + \dfrac{1}{g}\dfrac{I_F g}{R_A}\dfrac{R_c^2}{R_G^2}\dfrac{R_{G2}}{R_{FG}}\right]}$$

$$\frac{dV_{2A}}{dt} = \frac{g}{W_K}\left(F_{DK}\sin(\theta + \phi) - F_{LK}\cos(\theta + \phi) + W_K\cos\theta \right) \tag{3}$$

$$I_F\frac{d\omega_F}{dt} = -W_{LOAD}R_F \tag{4}$$

$$\frac{d\theta}{dt} = \frac{-V_{2A}}{L_t} \tag{5}$$

$$\frac{d\gamma}{dt} = \frac{-V_A}{R_A} \tag{6}$$

10 MATLAB Dynamic Simulation Results

The project team ran the MATLAB simulation for both of the kites utilized throughout the development of the kite power system. The main parameter changes between the two runs were the area of the kites and the weight of the kites. These runs were completed with the overall gear ratio of 6:1 and flywheel size (45 lbf weight plate) present on the actual system. The team was mainly interested in three outputs: potential power production, kite motion and tether tensions. The tether tensions were of interest because they would be used to for a Finite Element Analysis in CosmosWorks on the rocking arm. For this reason, the tensions for the 10 m^2 kite would be used as it was the kite that would pull with the most force.

10.1 Power Output

The instantaneous power output for the 10 m^2 and 6 m^2 kites are shown in Figure 40 and Figure 41, respectively. The graphs show an approximately 15 second interval from the middle portion of the run. This interval was chosen to allow transients in the start up of the system to steady out. One can clearly see the cyclic nature of the system, visible in the peaks and valleys of the graphs. The power produced by the 10 m^2 kite oscillates between about 2.2 kW and 3.2 kW, while the power produced by the 6 m^2 kite ranges from just over 1 kW to about 2 kW. The average power output, over all the cycles, for the larger kite is 2.82 kW, while the smaller kite produces about 1.67 kW. Both of these numbers are on par with what is expected to be produced, as other effects such as friction in the gearing and heat dissipated in generator would lower the power actually produced in the actual system.

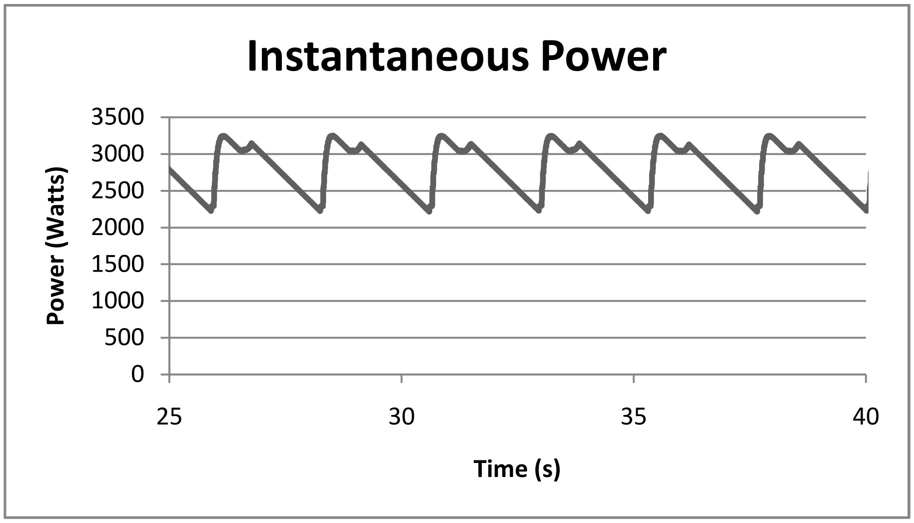

Figure 40: Instantaneous Power - 10m^2 kite

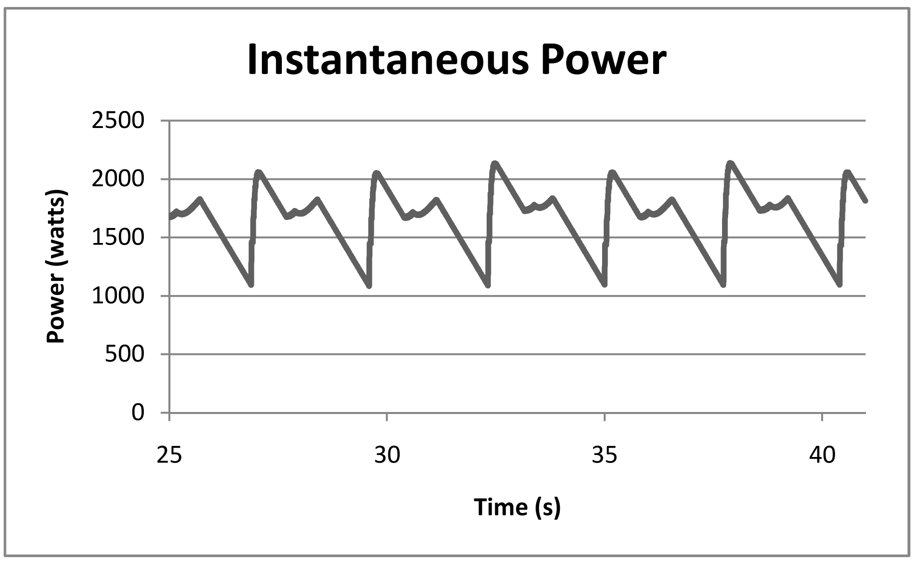

Figure 41: Instantaneous Power - 6m^2 kite

10.2 Kite Motion

The horizontal and vertical motion of the 10 m^2 and 6 m^2 kite during the simulation are shown in Figure 42 and Figure 43, respectively. This is the motion an observer would see if they were looking at the system from the side (similar to Figure 39 shown earlier). The path on each graph shows the relative movement of the kite; each kite begins the simulation at the origin (0,0) and moves from there. The motion shown for each kite is the stable loop each kite eventually enters after several cycles. It is interesting to note the different positions the kite enter their stable loops in, with the larger kite sitting more in front of the rocking arm than the smaller kite.

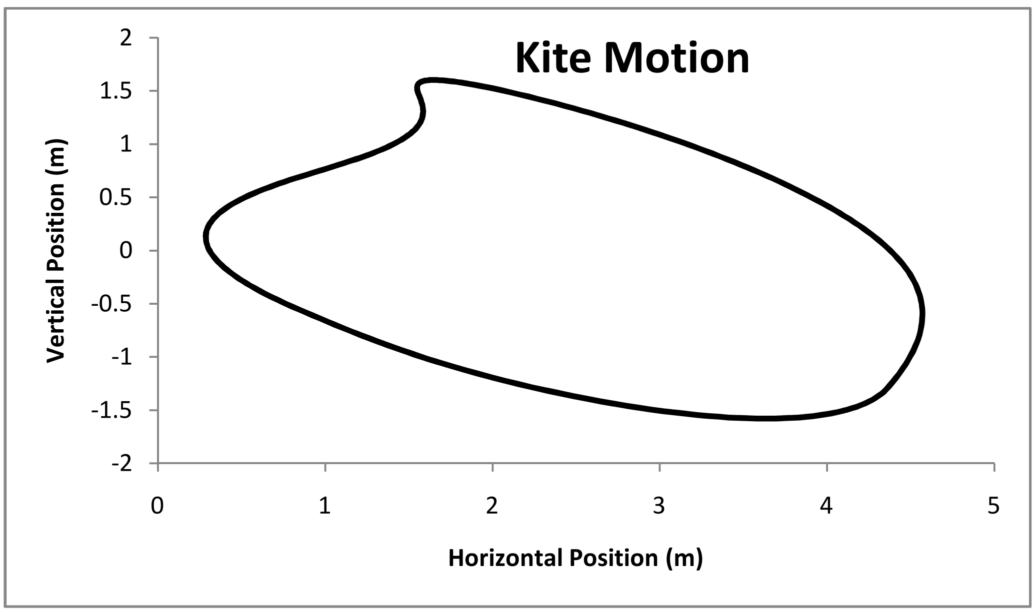

Figure 42: Motion of 10 m^2 kite

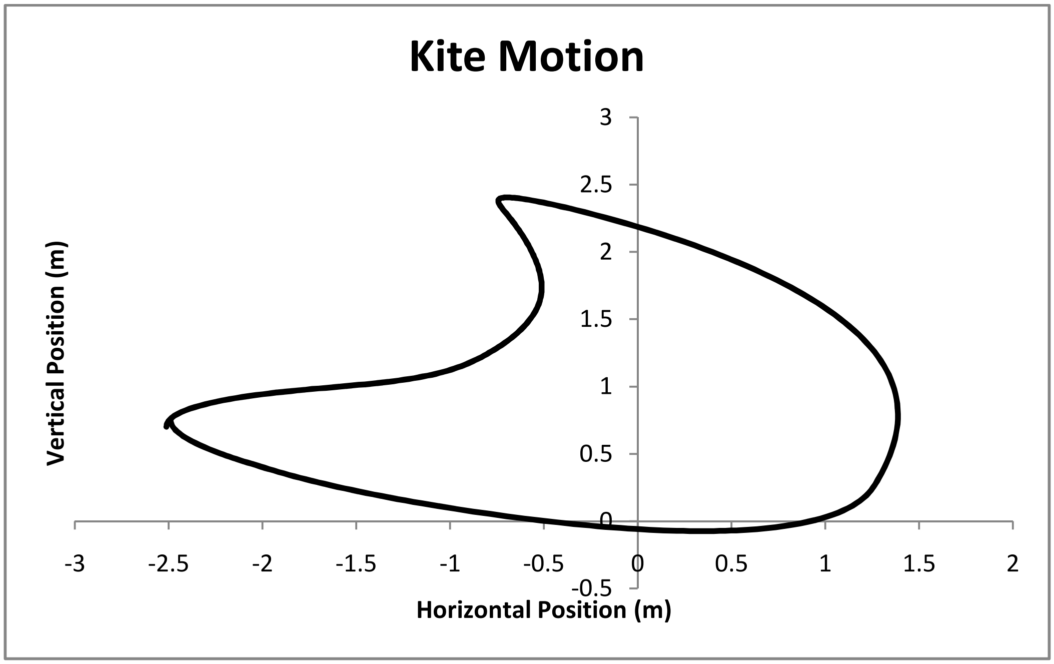

Figure 43: Motion of 6 m^2 kite

10.3 Tether Tensions

As previously mentioned, the MATLAB simulation was also used to determine anticipated tether tensions to use in a CosmosWorks Analysis on the rocking arm. These results from the MATLAB simulation are summarized in the CosmosWorks Section of the report.

11 CosmosWorks Finite Element Analysis

To ensure that the rocking arm would be able to withstand the loads placed on it by the kite during normal operation, a rough Finite Element Analysis was conducted using the CosmosWorks add-in for SolidsWorks. A solid model was completed of the three individual sections of the rocking arm and the individual components were put together in an assembly. The material for the arm was 6063-T6 Aluminum and a standard mesh was used. The constraints and loads placed on the beam can be seen in Figure 44.

The pink arrow closest to the center of the arm represents the force of the cord where the power conversion system is attached. The two pink sets of arrows toward the end of the arm represent the force from the kites tether lines. One force is perpendicular to the arm and one is parallel to the arm because the kite tethers pull at an angle to the beam. These two forces allow for the force to be decomposed into its components. The green bundle of arrows in the center of the arm shows that all six degrees of freedom in that location are constrained. This was acceptable for a simple analysis, as the arm was going to be examined separately at four different positions of the beam.

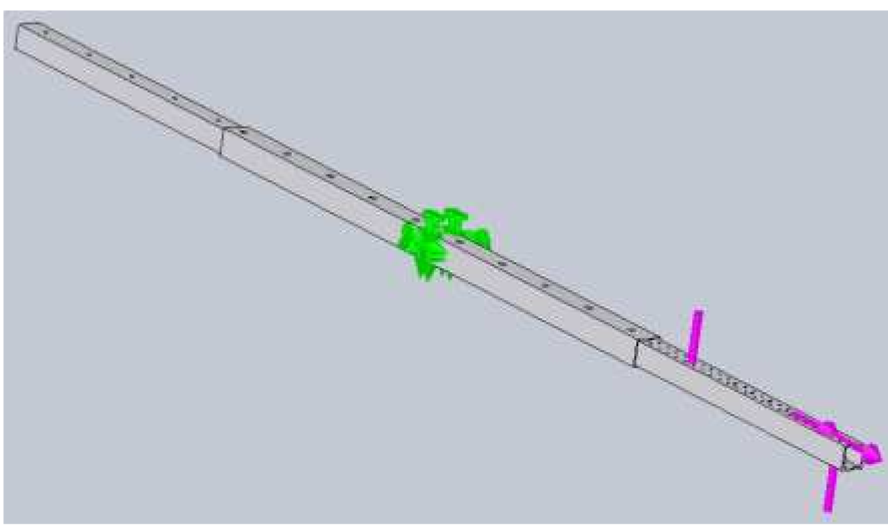

Figure 44: CosmosWorks Constraints and Loads

The four positions of the beam the project team wished to look at were: arm at the bottom of its stroke, arm at the horizontal position on ascent, arm at the top of its stroke as the angle of the attack of the kite is changed and arm at the horizontal position on descent. The kite tether tensions and angles were taken from the dynamic simulations conducted in MATLAB and the cord tension was calculated from a moment equilibrium on the arm, representing a situation where the beam is moving at a constant angular velocity.

12 CosmosWorks Finite Element Analysis Results

The summary of the loads from the MATLAB simulation us in the CosmosWorks cases are summarized below in Table 2. The most extreme case was when the arm is at the bottom of its stroke. This high spike is only for a very short time due to the quick deceleration of the beam, but is nonetheless an important case to look at.

Table 2: CosmosWorks Cases

Case	Kite Line Tension (lbf)	Cord Tension (lbf)	Angle (deg, wrta)	F_n (lbf)	F_p (lbf)
Lowest Beam angle (max condition)	**766**	**1099**	97	760	-97
Horizontal on Ascent	**106**	**143**	68	99	40
Just before AOA change	**181**	**182**	44	126	130
Horizontal on Descent	**28**	**35**	60	24	14

12.1 Von Mises Stress

The stress results from the CosmosWorks analysis are shown in Figure 45 through Figure 48. The arm in each figure is shown with a deformation scale of 4, but each stress scale is different in order to better visualize the stress distribution in the arm. The largest stresses are seen in the case 1 (bottom of the arm's stroke - Figure 45). In this figure, the top of the stress scale is set to be the yield strength of the material, 32 ksi. This is by far the highest load case and the stresses are still well below the yield stress of the material. The maximum stress seen in the beam is about 10 ksi where the two sections of the arm fit together. The other cases show that the stresses are relatively low for the other positions of the arm, confirming that the arm should be able to take the forces due to the kite and normal operation of the system.

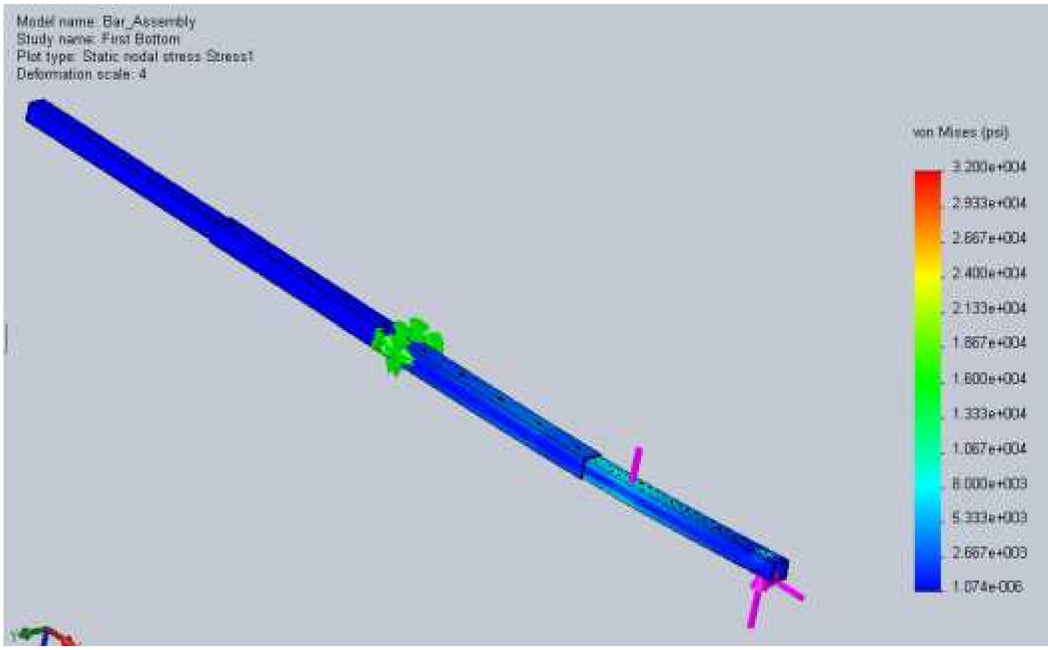

Figure 45: Von Mises Stress, Bottom of Stroke

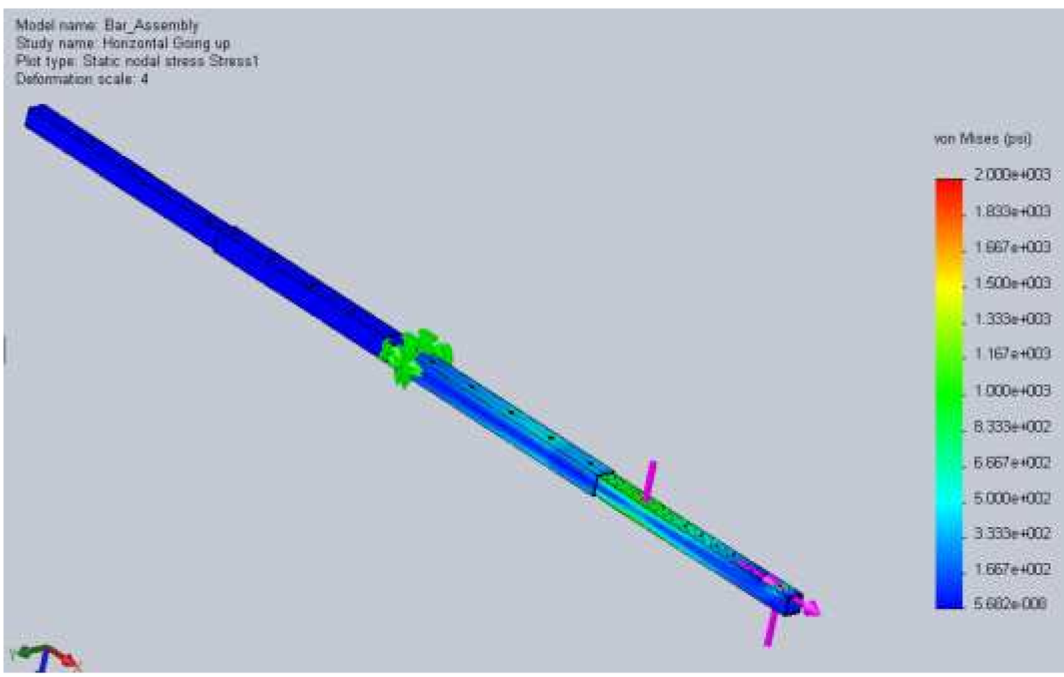

Figure 46: Von Mises Stress, Horizontal Ascent

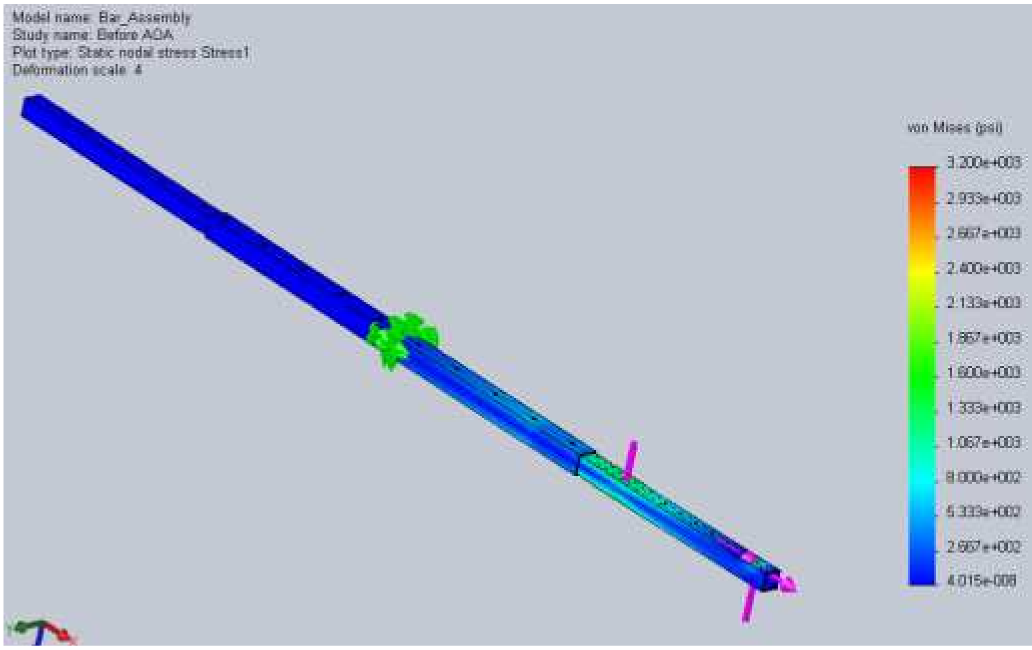

Figure 47: Von Mises Stress, Just Before AOA Change

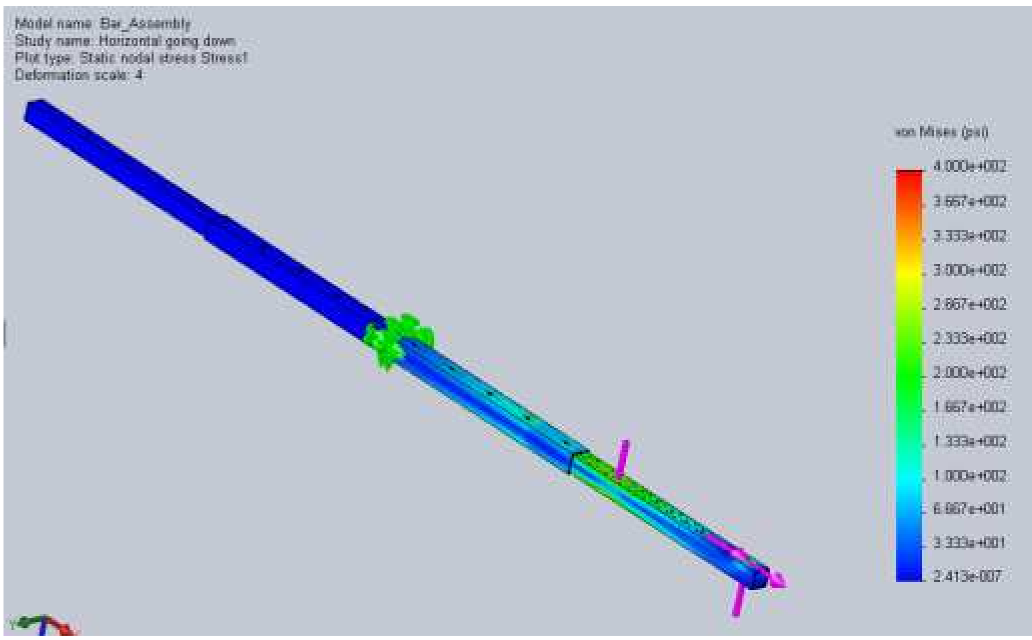

Figure 48: Von Mises Stress, Horizontal Descent

12.2 Displacement

The displacement results from the CosmosWorks analysis are shown in Figure 49-Figure 52. The deflection scale for all of the figures is once again 4 and overall the displacement of the beam under normal operation is very low. The highest displacement occurred on case 1 and was a mere .93 inches at the end of the arm. This is very low considering that the arm is about 7 feet long. All of the other deflections were less than ¼ inch. These results further confirm that the forces imposed on the beam are acceptable.

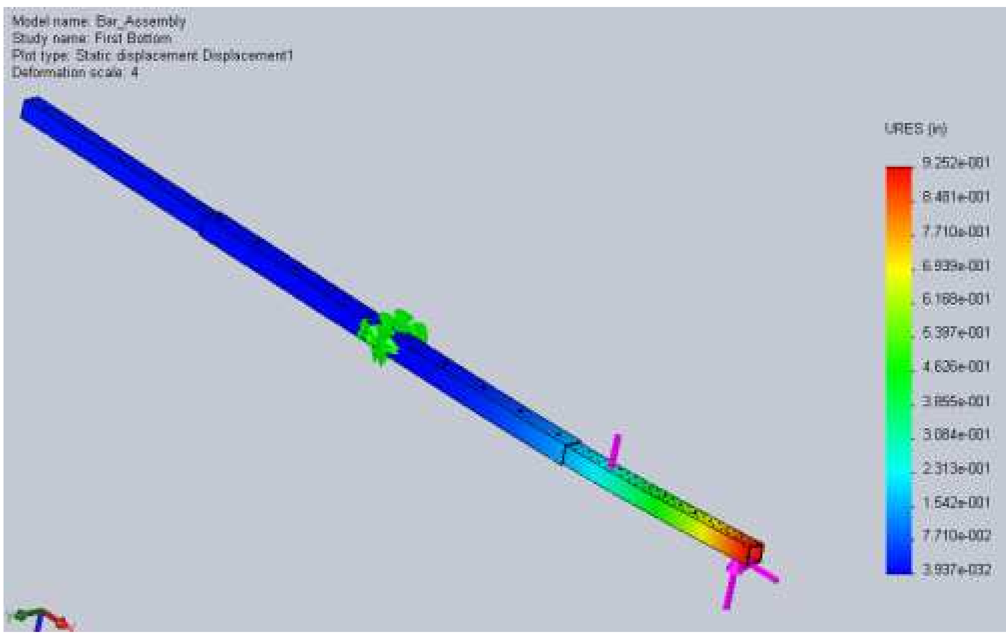

Figure 49: Deflection, Bottom of Stroke

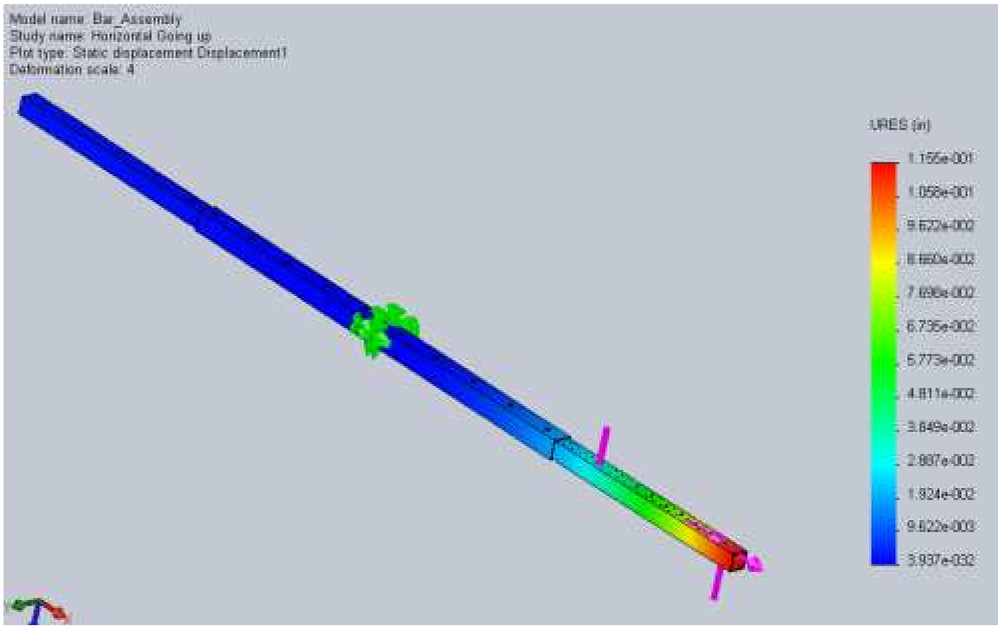

Figure 50: Deflection, Horizontal Ascent

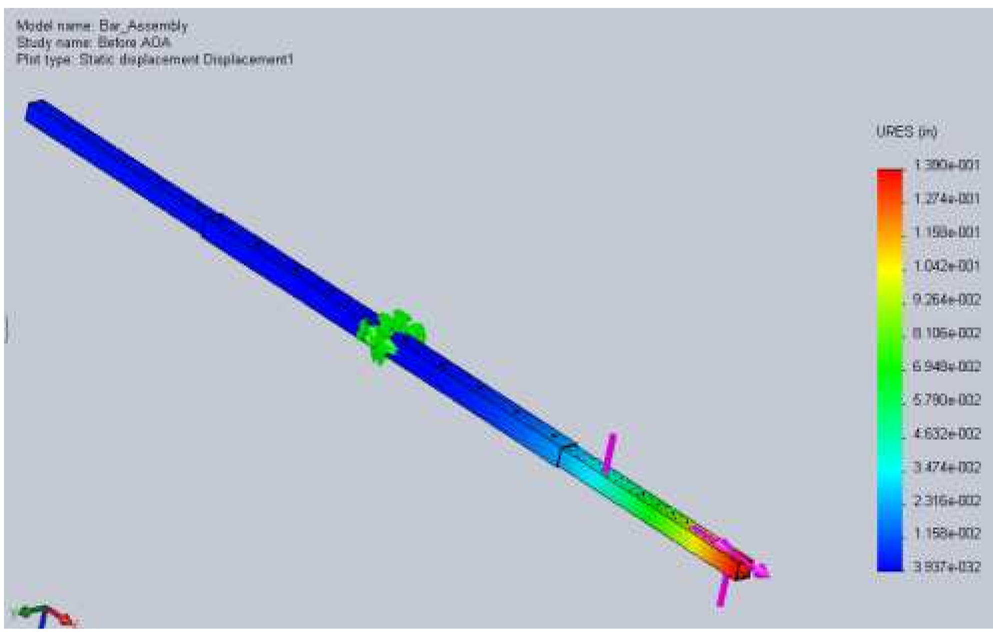

Figure 51: Deflection, Just Before AOA Change

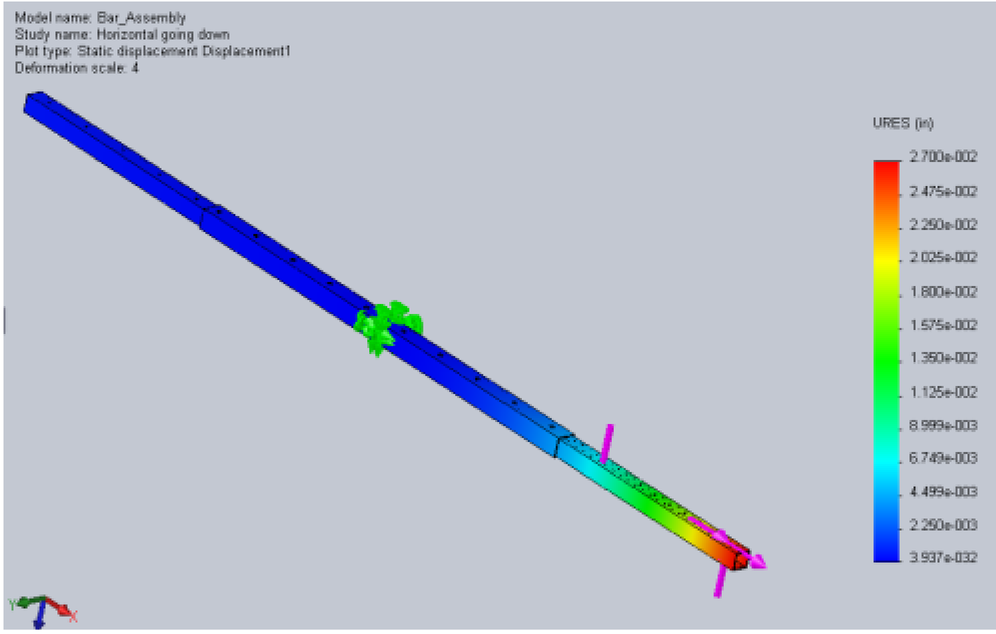

Figure 52:Deflection, Horizontal Descent

13 Conclusions

By the end of this project, we successfully utilized kites to harness wind power to show that it is feasible and in fact a very desirable way to produce power. We were able to design a kite control mechanism which autonomously could keep the kite flying for several minutes. Overcoming this challenge was very significant because it proves that a kite will remain in the air with no input. Although time restraints prevented us from attaching the angle of attack apparatus to the kite, we are confident that our flexible design would be able to properly perform its function. These developments demonstrate a kite power system which can harness power. To convert the power into usable electricity, we developed a powertrain to convert the mechanical energy into electrical energy. We also rigorously lab tested every component of the system to ensure that it they could sustain the required loads. One major problem that we encountered was addressing the problem of a sudden loss of wind. We conducted several low-level experiments with helium balloons to keep the kite afloat but soon realized that a deeper investigation into the problem was necessary.

Our final test, resulting in an electrical output with the kite attached, proved that this type of system can work. Considering the current global state of energy, it is noteworthy that we have developed a functional prototype for harnessing a sustainable, clean, cheap energy. We anticipate that future work in this area will yield excellent results.

On April 20-22, our MQP group will be presenting this project to the Environmental Protection Agency during their fourth annual National Sustainable Design Expo. There, we will be competing to get Phase II funding for the project. This funding would be used to further develop the prototype and implement a functional wind power system in Namibia, Africa.

13.1 Overall Results

- Developed a working kite power demonstrator
  - Roll stability
  - AOA change
  - Power conversion
- Rigorous lab and field testing
- Cosmosworks stress analysis
- Matlab simulation predicting system output
- Proved that kite power is a feasible, renewable, energy technology

Figure 53: Main poster for EPA conference

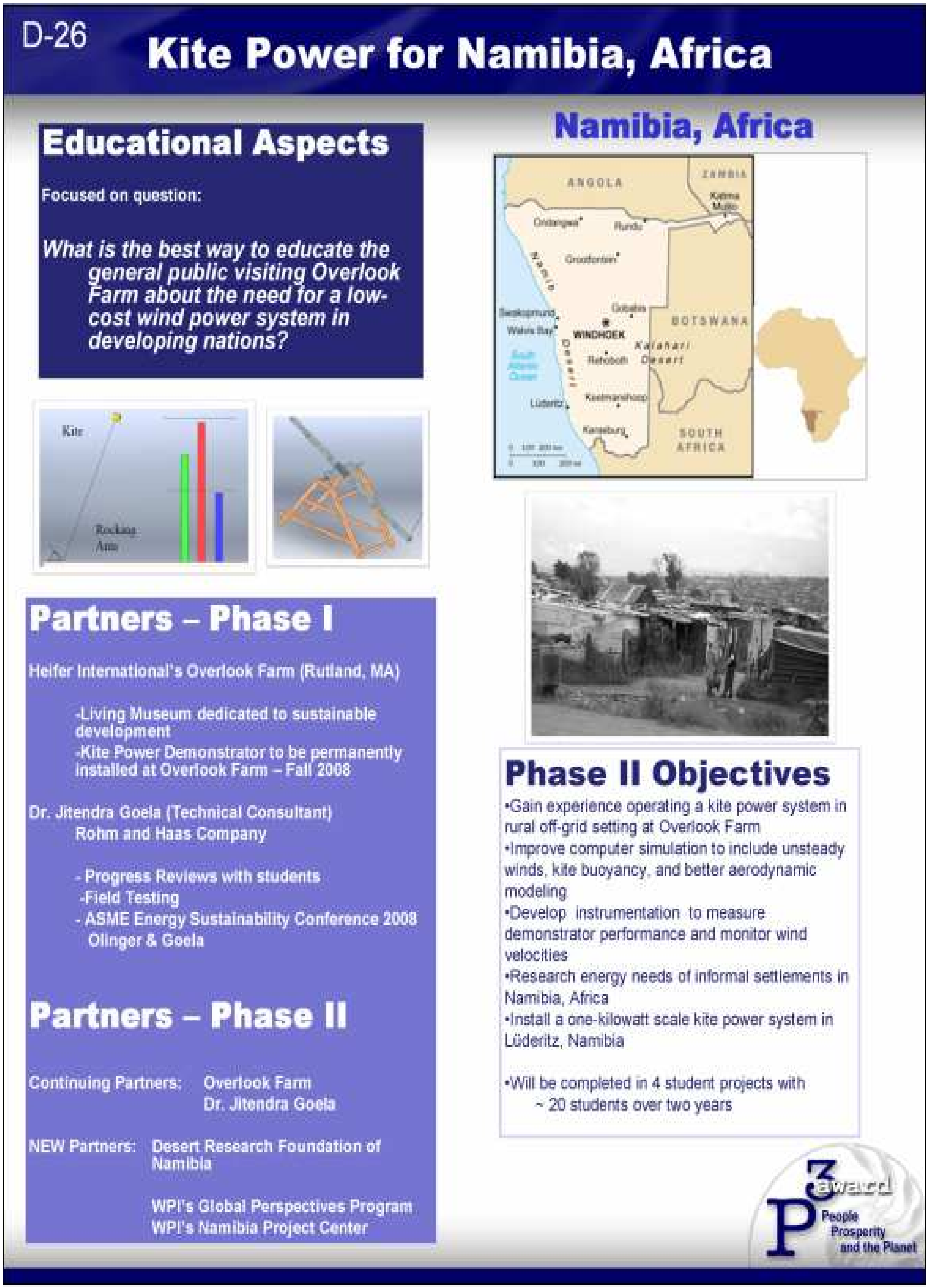

Figure 54: Supplementary poster for EPA conference

14 Future Work

Despite the great strides made by the project, many opportunities remain to continue to develop and improve the kite power concept. The primary goal for future work should be to fully achieve the objective of autonomous kite generated electricity. Further field testing is required, in which the beam would be allowed its full range of motion. Initially, a system for manually controlling the kite should be used. Eventually, the kite control systems should be developed to the point where they are capable of keeping the kite in the air while going through cycling between powered and depowered modes. The lateral kite control mechanism is currently capable of keeping the kite in the air for short periods of time and should be sufficient for initial testing. More testing needs to be done to determine when the angle of attack needs to change in order to power and depower the kite at the appropriate time. The angle of attack mechanism then needs to be developed so that it can use this information to run the kite through the power cycle.

An intermediate goal would be to modify the current system to allow for an operator to manually control the kite from a safe location, such as a “cockpit” built into the A-frame itself. This should be far simpler than autonomous power generation, as it removes the complexities of trying to control the kite using mechanical systems. This type of system would allow a user to generate power as needed, be it to charge batteries for a specific use or for tasks such as water pumping and grain milling.

Further research and development also needs to be done to improve the longevity of the system. Most of the current components were built as prototypes to test specific ideas and designs. These systems need to be refined and likely redesigned in order to improve their durability. In order to compete with options such as wind turbines, the system needs to be able to generate power continuously for extended periods of time with minimal maintenance.

Towards this end, more research must be done to find a method of keeping the kite in the air during periods of minimal wind. The use of lighter than air substances such as helium to keep the kite aloft were examined as part of this project, but further research is required to determine the feasibility of this option.

Work can also be done to improve computer simulations of the kite dynamics. Specifically, a better aerodynamic model of the kite is necessary as well as the modeling of additional effects such as unsteady winds. The simulation can also be improved by gathering more accurate data for the inputs in the model. This can be done by using more sophisticated instruments to measure tether line tension, rocking arm angles, shaft rotation and power output.

Once a fully functional system is developed, more work can be done to develop the system and prove the concept in an actual working environment. An ideal location for this work would be WPI's project center in Namibia, Africa. Namibia is in great need of the low-cost, clean electricity this system is designed to generate. The WPI project center focuses largely on sustainable development and would be well suited to sponsor the installation and operation of a kite power system. These are just some of the opportunities for continuing the work done by this project.

15 Reference List

[1] http://www.scoop.co.nz/stories/HL0505/S00054.htm

[2] http://www.ren21.net/globalstatusreport/download/RE_GSR_2006_Update.pdf

[3] http://www.eia.doe.gov/emeu/aer/overview.html

[4] http://www.ninapierpont.com/pdf/Health_effects_of_wind_turbine_noise_3-2-06.pdf

[5] http://www.scoop.co.nz/stories/HL0505/S00054.htm

[6] Olinger D., Goela J.S., "Performance Characteristics of a One-Kilowatt Scale Kite Power System", Proceedings of Energy Sustainability, 2008

[7] http://www.wpi.edu/Pubs/E-project/Available/E-project-042607-112625/

[8] Loyd, M.L., 1980, "Crosswind Kite Power", J. Energy, 4(3), pp 106-111.

[9] Goela, J.S., 1979, "Wind Power Through Kites", Mech. Engg

[10] Goela, J. S., 1983, "Project Report II on Wind Energy Conversion Through Kites", DST Project Report No. DST/ME(JSG)/81-84/26/2, IIT Kanpur.

[11] Goela, J.S., Vijaykumar, R. and Zimmermann, R.H., 1986, "Performance Characteristics of a Kite-Powered Pump", J. Energy Resource Tech

[12]Lang et al., "Electrical Power Generation Using Kites", 2005

[13] http://www.youtube.com/watch?v=0BOdLbQN36Q

[14] http://www.weather.gov/forecasts/graphical/sectors/massachusetts.php#tabs

[15] http://www.youtube.com/watch?v=0BOdLbQN36Q

[16] http://www.youtube.com/watch?v=10JMr_3UN0g&feature=related

[17]http://www.youtube.com/watch?v=IHim2Vnkikw&feature=related